ACS Chemical Neuroscience
Cite This: ACS Chem. Neurosci. 2018, 9, 2074−2088
Research Article
pubs.acs.org/chemneuro

# Immunohistochemical Approach to Understanding the Organization of the Olfactory System in the Cuttlefish, *Sepia officinalis*

Alexia T. Scaros,[†] Roger P. Croll,[†] and Sébastien Baratte*[,‡]

[†]Department of Physiology and Biophysics, Dalhousie University, Halifax, Nova Scotia B3H 4R2, Canada
[‡]Sorbonne Université, MNHN, UNICAEN, UA, CNRS, IRD, Biologie des Organismes et Ecosystèmes Aquatiques (BOREA), Paris 75005, France

**ABSTRACT:** Cephalopods are nontraditional but captivating models of invertebrate neurobiology, particularly in evolutionary comparisons. Cephalopod olfactory systems have striking similarities and fundamental differences with vertebrates, arthropods, and gastropods, raising questions about the ancestral origins of those systems. We describe here the organization and development of the olfactory system of the common cuttlefish, *Sepia officinalis*, using immunohistochemistry and in situ hybridization. FMRFamide and/or related peptides and histamine are putative neurotransmitters in olfactory sensory neurons. Other neurotransmitters, including serotonin and APGWamide within the olfactory and other brain lobes, suggest efferent control of olfactory input and/or roles in the processing of olfactory information. The distributions of neurotransmitters, along with staining patterns of phalloidin, anti-acetylated α-tubulin, and a synaptotagmin riboprobe, help to clarify the structure of the olfactory lobe. We discuss a key difference, the lack of identifiable olfactory glomeruli, in cuttlefish in comparison to other models, and suggest its implications for the evolution of olfaction.

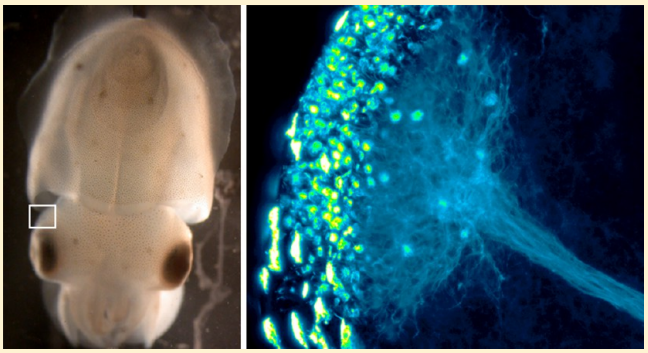

**KEYWORDS:** *Cephalopod, olfaction, glomerulus, neurotransmitters, immunohistochemistry, in situ hybridization*



## INTRODUCTION

While not generally considered traditional models in neuroscience, cephalopods have nonetheless long been subjects of intense curiosity in both the scientific and lay communities.[1] As members of the phylum Mollusca, their lineage split early from those of the more widely studied vertebrates and arthropods; yet, cephalopods exhibit similar degrees of intelligence, mobility, and environmental adaptation though framed in a fundamentally different morphology. This unique evolutionary history and unusual combination of traits has inspired studies of cephalopod anatomy and physiology for over a hundred years.[2] During his work in the 1930s, Young described many characteristics of cephalopods, such as giant axons, which later provided a foundation for Hodgkin and Huxley's Nobel Prize on the ionic basis of action potentials.[3,4] Other renowned pioneers of modern cephalopod neuroscience include Messenger, who mapped the central nervous systems of several species, and Wells, who explored behavioral aspects of cephalopod neuroscience.[5,6]

Comparing the nervous systems of various lineages throughout the animal kingdom is useful for understanding the evolutionary history of these systems. For example, cephalopods rely heavily upon vision for prey detection, predator avoidance, and social interactions. Previous comparisons of their visual systems with those of other animals have provided powerful insights into the evolution of eyes and how the brains of these animals are organized to mediate their remarkable intelligence.[7−9] It can therefore be expected that comparisons of other sensory systems might prove to be equally fruitful. However, as Eisthen[10] suggests, it can be difficult to distinguish the point of diversion between similar model systems in evolutionary history. Two possibilities are (1) that any similarity across multiple models may reflect a common basic biological solution that is favored and efficient and therefore occurs repeatedly throughout evolution (convergence) or, alternatively, (2) that certain systems arose once in an early ancestor and were passed down through evolution (homology).

The mechanisms underlying the olfactory systems among different model species appear to follow common patterns despite the apparent diversity of external olfactory organs (Olf Os; e.g., the antennae of insects or nostrils of vertebrates). Odorant molecules bind to olfactory receptors (either G protein-coupled receptors[11] or ligand gated ion channels[12]) generally found on ciliated olfactory sensory neurons (OSNs). Located in a specialized olfactory epithelium (Olf E) within the

**Special Issue:** Model Systems in Neuroscience

**Received:** January 17, 2018
**Accepted:** March 26, 2018
**Published:** March 26, 2018




DOI: 10.1021/acschemneuro.8b00021
ACS Chem. Neurosci. 2018, 9, 2074−2088

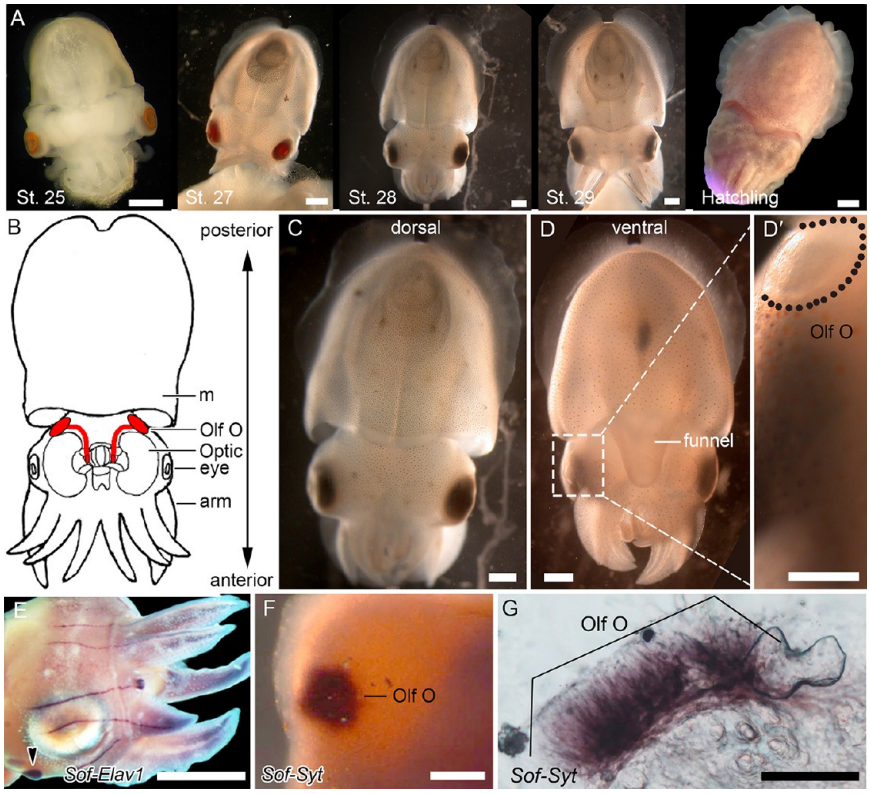


**Figure 1.** Developmental stages and olfactory system in *Sepia officinalis*. (A) Mid- to late-embryonic development. Stage 25 is identifiable based on the light orange eyes and T-shape formed by the head and mantle. At stage 27, the eyes are red/brown, the head has begun to round, and the cuttlebone is visible with two rings of calcium deposits. The first chromatophores are visible around stage 28. During this time, the eyes are a dark brown/black color, the head and mantle have taken on their final shape, and the cuttlebone has three rings. Through stage 29, chromatophores continue to multiply and are more pronounced, eyes begin to have iridescence, arms elongate, and the cuttlebone develops four rings. Approximately one week after hatching, the skin is no longer transparent and the overall morphology resembles a small adult. (B) A diagrammatic representation of the cuttlefish embryo shows the location of the central nervous system and olfactory system (red). (C) In a dorsal view of a stage 29 embryo, the posterior end is at the tip of the mantle and the anterior end is at the tip of the arms. (D) The same embryo is seen from a ventral view; water flows into the mantle above the olfactory organ, which is located posterior and ventral to the eye (rectangle). Water is then ejected out the funnel. (D′) Magnified view illustrates the olfactory organ (circled) posterior to the eye and anterior to the mantle on the ventral side of the head. (E) In situ hybridization with *Sof-Elav1* riboprobe demonstrates expression in the lateral lines and the olfactory organ (arrowhead) from a lateral perspective facing the right eye. (F) *Sof-Syt* riboprobe in whole-mount shows a tight cluster of cell bodies in the olfactory organ and the absence of nearby cell bodies in the head epithelium. (G) Section of the olfactory organ (bracket) from a stage 26 embryo with in situ hybridization staining using a *Sof-Syt* riboprobe revealed labeled cells that extend from the neuropil to the subepithelium. m, mantle; Olf O, olfactory organ; *Sof-Elav1*, *Sepia officinalis-Elav1*; *Sof-Syt*, *Sepia officinalis*-synaptotagmin. Scale bars: A, C, D, E = 1 mm; D′, F = 500 $\mu$m; G = 100 $\mu$m.

Olf O, these OSNs generate action potentials that travel into an olfactory center of the brain (olfactory bulb in mammals[13] or antennal lobe in insects).[14,10] In some animal groups, olfactory glomeruli, composed of tightly clustered OSN axonal terminals and dendrites, are located at the junction of the afferent fibers and the higher brain centers. Since each glomerulus only receives sensory inputs from OSNs expressing the same receptor protein, this structure has been suggested to be an optimal solution to discriminate odors and enhance signal detection.[11,10,15] Olfactory glomeruli have been studied extensively in Vertebrata (particularly mammals, fish, and amphibians) and Arthropoda (including insects, crustaceans, and onychophorans).[10,15] Even some annelid species have been described as having mushroom bodies with clustered, spheroid neuropil akin to olfactory glomeruli.[16] However, the presence of olfactory glomeruli in Lophotochozoa remains uncertain. To determine whether the presence of glomeruli is a homologous feature shared among most animal groups or an optimal solution that evolved convergently at least twice, the presence of olfactory glomeruli in molluscs needs to be ascertained. Because of their well-developed sense of smell and highly cephalized nervous systems, molluscs are more comparable to other species than their simpler vermiform cousins. Investigations of the olfactory systems of molluscs to date have mostly been conducted in gastropods, which are able to use chemical cues to find and discriminate between foods.[17,18] Numerous studies have also described possible glomeruli in the olfactory pathways of these animals.[19−26,18] However, several characteristics of these structures suggest that molluscan glomeruli differ fundamentally from those of vertebrates and arthropods[19] and raise questions regarding assumptions of homology. For example, while glomeruli in vertebrates, insects, and crustaceans are found in their respective olfactory centers within the central nervous system, gastropod glomeruli have been reported in the periphery directly beneath the Olf E in snails and slugs.[19,21−23,25,18] Additionally, there seems to be far fewer glomeruli in gastropods; only 20 olfactory glomeruli were reported in a land snail in comparison to 125 found in a species of cockroach or almost 2000 found in a rabbit.[19] Gastropod glomeruli also seem to be more irregularly shaped in comparison to the more spherical morphology found in other clades. Finally, the snail glomeruli only receive a small portion


DOI: 10.1021/acschemneuro.8b00021
ACS Chem. Neurosci. 2018, 9, 2074−2088

of olfactory afferent projections, while the rest bypass the glomeruli. This limited input into the glomerulus is another deviation from both vertebrates, which route almost all their neurites through glomeruli,[27] and arthropods, which route most of their inputs through glomerular neurites. With all the ambiguity surrounding gastropods, comparisons with another class might clarify the presence of olfactory glomeruli in molluscs. With their high degree of cephalization and large brains, cephalopods can elucidate our understanding.

Cephalopods appear to use olfaction to identify and target prey as they have been observed to move toward stimulatory chemicals (e.g., amino acids) and "fish juice."[5,30] In addition, cephlopods have demonstrated an aversion to chemicals including tetraethylammonium, tetrodotoxin, squid ink, and the odors of predators.[28−31] Olfaction has even been suggested to play a role in social communication.[31] The Olf Os of cephalopods are diverse: nautiluses have protruding rhinophores,[32,33] while coleoid cephalopods (squid, octopus, and cuttlefish) have internalized pits.[34] The ciliated sensory neurons in the Olf Os of coleoids project their axons via an olfactory nerve to a distinct olfactory lobe that sits along the optic tract.[35] While the olfactory lobes of *Nautilus*[36] and *Octopus*[37] have been previously described using classical silver staining techniques, there has never been mention of structures remotely resembling a glomerulus. However, these cephalopod studies were conducted before glomerular structures were defined according to modern criteria (see below). Therefore, it is possible that such structures might have been overlooked or unidentified in the past. In addition to these past descriptions of *Nautilus* and *Octopus*, Messenger also described the structure of the olfactory lobe in squid *Loligo*[6] but admitted that "cells in the olfactory lobe are rarely impregnated after staining by the Golgi method, so little is known of their form... the axons are not well-defined" (p. 298). This admission demonstrates the need for the use of updated methods to describe the neurotransmitters present in the olfactory system of cephalopods. While there have also been more recent studies on the olfactory system in *Octopus*, no glomeruli have been identified.[38−40]

In this study, we focus on the structure of the olfactory system of the cuttlefish *Sepia officinalis* at late embryonic and hatchling stages of development. To mark differentiated neurons, we used riboprobes for the synaptotagmin (*Sof-Syt*[41]) and *Elav1* (*Sof-Elav1*[42,43]) genes. To follow axons in the olfactory nerve and throughout the olfactory system, we used DiI[44−46] along with antibodies against acetylated $\alpha$-tubulin (prevalent in axons[35,47−49,42]). To observe growing neurites, we used phalloidin to stain filamentous (F)-actin.[50,51,48] We also examined the distributions of a variety of neurotransmitters and neuropeptides (references provided below) that have been either identified or implicated in putative olfactory centers in molluscs, including cephalopods: FMRFamide (FMRFa; Phe-Met-Arg-Phe-$NH_2$) and related peptides (FaRPs), serotonin (5-HT), APGWamide (APGWa; Ala-Pro-Gly-Trp-$NH_2$), histamine (HA), and nitric oxide synthase (NOS). These techniques were used to improve upon past descriptions, clarify current controversies, and supply new evidence to answer questions regarding the evolution of glomeruli using a novel model system in cuttlefish embryos.

## RESULTS AND DISCUSSION

**Development and Morphology of the Olfactory Organ.** As direct developers, cuttlefish progress from a thin layer of embryonic cells atop a yolk into their adult morphology without a larval stage (Figure 1A). The Olf Os of embryonic *S. officinalis* consist of clusters of sensory cells located posterior-ventrally to the eyes on each side of the head (Figure 1B−D′). Stages 14−20 are considered the placode stages, in which the ectoderm organs (including the Olf O) develop.[52] The OSNs have been observed to differentiate around stage 16[42] and can be revealed by the labeling of *Sof-Elav1*, an early genetic marker of neurons, using in situ hybridization (ISH) (Figure 1E, arrowhead). ISH also revealed expression of the *Sof-Syt* gene[41] that codes for synaptotagmin, a synaptic protein in mature synapses beneath the surface of the Olf E (Figure 1F, G).

The Olf O, including its underlying neuropil, and the olfactory nerve were identifiable by anti-acetylated alpha ($\alpha$)-tubulin (AcTub) immunohistochemistry (IHC) when examined at stage 25 (Figure 2A). At this time, numerous, brightly stained, and generally spheroidal structures with a mean diameter of 6 ± 2 $\mu$m ($n$= 19 specimens) were also apparent immediately beneath the surface of the Olf E (Figure 2A). The Olf O at stage 25 averaged 335 ± 36 $\mu$m in diameter ($n$ = 8).

At stage 29 of development, the diameter of the Olf O increased to an average of 429 ± 116 $\mu$m ($n$ = 15). By this time, the tubulin-rich, small spheroidal structures just beneath the surface of the Olf E had become more numerous and clearly differentiated the Olf O from the surrounding body wall, which was covered by larger tufts of long cilia (Figure 2B, C, arrowheads; also see ref 42).

Closer inspection of the Olf O at stage 30 revealed a complex Olf E with what appeared to be numerous cell types labeled by anti-AcTub (Figure 2D). Deep within the Olf E lay cell bodies with variously shaped projections extending toward the surface. Some of these projections appeared to have swellings at their apical ends (asterisks), while others tapered into fine tips (arrows). Just beneath the surface of the Olf E were smaller spheroidal structures (Figure 2D). A carpet of free cilia overlay the surface of the Olf E. Double-labeling with phalloidin at this stage revealed that muscle fibers lay underneath the organ but none penetrated the organ itself (Figure 2D). Many of the cell bodies in the Olf O possessed a concentration of F-actin at their apical poles (Figure 2D insert, arrowheads). This complex Olf E, with what appears to be multiple cell types, is consistent with previous descriptions of Olf Os in other cephalopods.

Sensory neurons were originally described in the chemoreceptive rhinophore of *Nautilus*[32] and the Olf O of *Octopus*.[34,53,54] Both structures were found to possess multiple types of bipolar, ciliated OSNs. Emery[55] defined five types of sensory cell morphologies in the squid, *Lolliguncula*, which he described as more variable and complex than those previously noted in *Nautilus* and *Octopus* (Figure 3). Mobley et al.[30] estimated the abundance of each type of OSN in the squid Olf E with <1% being type I, ∼14% type II, and 20% types III−V, thereby leaving the remaining 66% as other nonsensory epithelial cells. In the Olf O of *Octopus*, five cell types have also been identified,[53,54] three of which were suggested to be OSNs. These descriptions of cell types were closely congruent to those previously described by Emery and Mobley in squid, except with fewer OSN types in *Octopus*.

Although our staining with anti-AcTub was consistent with the presence of numerous types of OSNs in the cuttlefish, views of individual OSNs were generally obscured by intermingled processes from neighboring cells. It was therefore difficult to recognize unambiguous profiles of any specific cell type, similar to those previously described in the squid.[55] The most prominent features of the Olf O seen here, and as first noted


DOI: 10.1021/acschemneuro.8b00021
ACS Chem. Neurosci. 2018, 9, 2074−2088

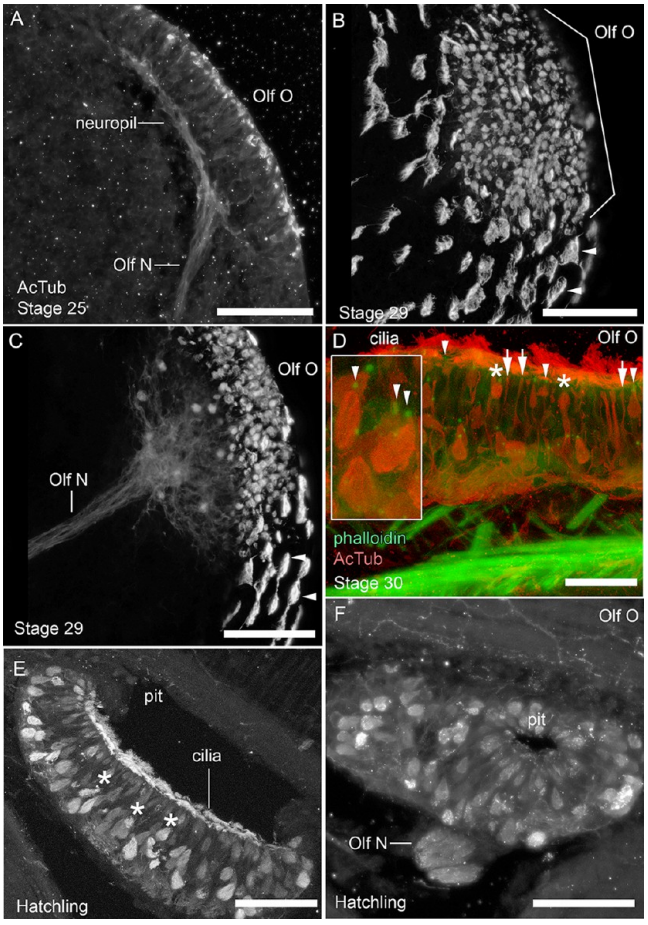


**Figure 2.** Acetylated $\alpha$-tubulin (AcTub) in the olfactory organ. (A) Section of the olfactory organ at stage 25 contains numerous, small, tubulin-rich elements immediately beneath the epithelial surface, a neuropil beneath the organ, and an olfactory nerve. (B) At stage 29, large tufts of cilia (arrowheads) surround the olfactory organ (bracket) with smaller, brightly stained, spheroidal elements beneath its surface. (C) View of the subepithelial structure of the olfactory organ demonstrates that the olfactory nerve projects from the organ toward the brain, and tubulin-rich elements sit beneath the olfactory epithelium. Arrowheads indicate examples of large tufts of cilia on the body wall surrounding the organ. (D) Double-labeling with anti-AcTub (red) and phalloidin (green) exhibits minimal colocalization. Anti-AcTub labels multiple cell body morphologies including some with projections that appear to have swellings at their apical ends (asterisks), while others tapered into fine tips (arrows). The cilia that line the lumen of the olfactory pit are also AcTub-positive. Brightly fluorescent punctata of F-actin (green, arrowheads) are consistently present at the apical tips of the cell bodies (red). The location of the F-actin punctata relative to the apical tips is more clearly demonstrated in the high magnification of the inset. (E) Section through the middle of a week-old hatchling's olfactory organ with the now invaginated epithelium forms a semitorus (half-doughnut shape) when sectioned at an angle. Cilia can be observed both lining the inside of the pit and as internalized cilia under the epithelium (asterisks). (F) Surface of a hatchling's olfactory organ that has been shallowly sectioned shows the opening to the olfactory pit. AcTub, acetylated $\alpha$-tubulin; Olf O, olfactory organ; Olf N, olfactory nerve. Scale bars: A–C, E, F = 100 $\mu$m; D = 50 $\mu$m.

by Buresi et al.,[42] were brightly labeled, tubulin-rich structures lying immediately beneath the epithelial surface that we interpret as being bundles of internalized cilia characteristic of types II, III, and IV OSNs.[53−55] In addition, the free cilia

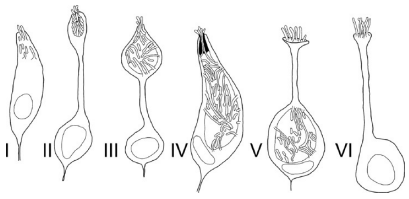


**Figure 3.** Olfactory sensory neuron morphologies. Diagrammatic representation based on an illustration published by Emery (1975) demonstrates the five cell morphologies of OSNs in cephalopods (I–V) and a sixth epithelial support cell type (VI).

overlying the surface of the Olf E likely derives from type V OSNs and type VI non-neural epithelial cells.

Due to the close positioning of cell bodies and processes in the Olf O, the techniques used here prevent accurate determination of cell densities at different developmental stages. Future experiments may rely upon nuclear stains or additional antibodies to obtain an approximation of the total cell density in the Olf O in order to speculate on the percentages of each cell type morphology.

An examination of hatchlings revealed no change in the diameter of the Olf O (Figure 2E), although its thickness had almost doubled from 65 ± 21 $\mu$m ($n$ = 24) at stage 29 to an average depth of 107 ± 14 $\mu$m ($n$ = 10) after hatching. In addition, the Olf E invaginated and formed the olfactory pit in the center of the surface of the Olf O (Figure 2E). The invagination seemed to occupy a large volume of the entire organ, with the Olf E thickness being only 94 ± 13 $\mu$m ($n$ = 3). After hatching, the Olf E had a pit opening 50 ± 11 $\mu$m ($n$ = 2) in diameter (Figure 2F), with a layer of what appeared to be internalized cilia (asterisks), and numerous free cilia that lined the lumen of the pit (Figure 2E). We speculate that the development of an olfactory pit, reminiscent of the vertebrate "nostril," may increase surface area of the Olf E, concentrate odorant in a semi-enclosed space, and/or protect OSNs from direct contact with the environment. Additionally, although there is not a complex F-actin network in the Olf O (not shown) that would suggest an intricate muscular system, most aquatic nostrils are able to dilate and constrict to control water flow.

Sensory systems appear to function as early as they develop morphologically in cephalopod organogenesis. In *S. officinalis*, embryos can react to tactile, chemical, and visual stimuli in ovo.[56,47,57] Cuttlefish embryos still in the egg capsule can respond to an aversive odorant, demonstrating that at least some components of their chemosensory system are functional even before hatching.[57] This behavior, in combination with the presence of the primitive Olf O and nerve at stage 25, suggests the embryo may have a rudimentary yet functional olfactory system at an early developmental stage. However, there are other chemosensory organs besides the Olf O that may be functioning before the olfactory system, including contact sensory cells on the suckers[58,5] or recently suggested sensory cells in the forehead.[59] Nonetheless, the increasing size of the Olf O and Olf E throughout development suggests an increase in OSNs and therefore a possible increase in the olfactory abilities of the embryos and hatchlings as they mature.

**Neurotransmitters in the Olfactory Organ.** *FMRFamide Related Peptides.* Anti-FMRFa has been widely accepted as labeling the family of FaRPs that all share an -RFamide sequence at their C-terminus.[60] In cephalopods, FaRPs are present in the olfactory system (*I. notoides*,[55] *S. officinalis*,[53,54]


DOI: 10.1021/acschemneuro.8b00021
ACS Chem. Neurosci. 2018, 9, 2074−2088

and *Octopus vulgaris*[61]). In *Sepia,* FMRFa-like immunoreactive (-LIR) staining showed numerous brightly labeled projections extending to the surface of the Olf E (Figure 4A). Closer inspection revealed more dimly labeled bipolar cell bodies (mean 8 ± 2 μm in diameter; $n$ = 11) with one strongly fluorescent apical neurite and another basal neurite that projected to the neuropil that underlay the Olf E (Figure 4A inset). The olfactory nerve was also visible in sections processed for anti-FMRFa (Figure 4A). However, faint and compartmentalized staining of the cells hindered our ability to assign them to a specific morphological type, although the slender apical processes seemed to be most consistent with cell types II, III and V described by Emery[55] and Polese et al.[54] ISH confirmed the presence of cell bodies that expressed the *Sof-FMRFa* gene in the Olf O of stage 27 embryos (Figure 4B, C, C′)

*Histamine.* Whole-mount IHC revealed that HA-LIR staining was isolated to the Olf O and not present anywhere else in the head or mantle epithelium. The most apparent features observed were small, intensely stained punctata, 2 ±1 μm in diameter ($n$ = 63) that were dispersed throughout the Olf O (Figure 4D, arrowheads). Higher magnification revealed that these punctata were consistently at the apical ends of faintly stained cell bodies (14 ± 2 μm in diameter; $n$ = 11; arrows) or along thin neurites extending to the surface of the Olf E (Figure 4D inset, arrowheads). Labeled axons were also present in the neuropil and in the olfactory nerve.

*Nitric Oxide Synthase.* NOS has been demonstrated to be present in the olfactory lobe of cuttlefish.[62,39] Our results show that NOS-LIR staining is present in the Olf O (Figure 4E), thus suggesting that a subset of OSNs might use nitric oxide for neurotransmission. NOS-LIR staining was confined to punctata interspersed between bundles of internalized cilia in the Olf O and no cell bodies were visible. The lack of identifying characteristics in the NOS-LIR staining prevented us from further speculating on the type of OSNs.

The finding of NOS, HA, and FaRPs in cuttlefish OSNs seems to follow a general molluscan plan. Nitric oxide has been suggested to be a neurotransmitter used by chemosensory neurons in other gastropods.[63,46] Similarly, HA has been described in the putative chemosensory neurons of several gastropod species.[64,46,65] FaRPs have previously been found in the Olf E of the terrestrial slug *Limax*[66] and in the chemosensory osphradium of the pond snail *Lymnaea*.[67] While the presence of these transmitters in the Olf O of *Sepia* is consistent with past literature on molluscan chemosensation, the reasons for the incomplete staining of neurons in the Olf O with transmitter-specific markers are not clear. Incomplete fixation, especially with the two-stage, EDAC-based fixative needed for anti-HA IHC (see below), could have contributed to our limited observations. Another possibility is that the antigens were strictly localized within presynaptic compartments, especially for the results involving NOS which might be used for transmission between cells within the Olf O.

Our results not only suggest possible transmitters used by OSNs in *Sepia* but also seem to exclude other candidate transmitters.

*APGWamide.* APGWa functions as a neurotransmitter peptide in gastropod central nervous systems, as well as in the central nervous system and peripheral axons of bivalves and cephalopods.[40] There were no APGWa-LIR cell bodies or neurites in the Olf O (Figure 4F), although the outer layer of the neuropil of the nearby optic lobe was intensely immuno-

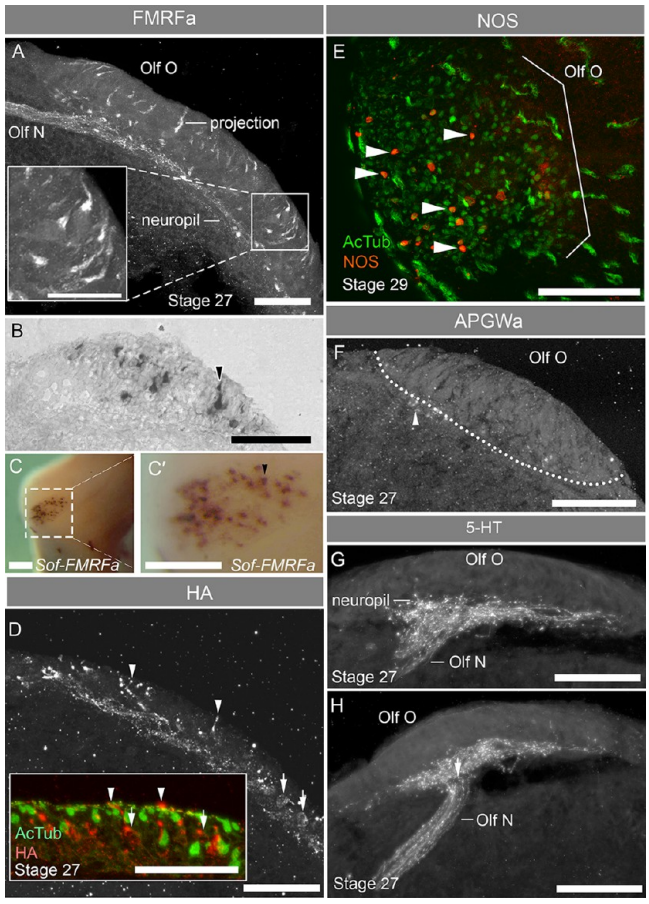


**Figure 4.** Neurotransmitters in the olfactory organ. (A) FMRFa-LIR bipolar cell bodies extend projections to both the surface of the olfactory epithelium and to the neuropil. The inset shows a high magnification of FMRFa-LIR staining in dimly fluorescent cell bodies with brighter apical projections. (B) Representative section through the middle of the olfactory organ stained with ISH shows *Sof-FMRFa* expressing cell bodies (arrowhead). (C) Staining with the Sof-*FMRFa* riboprobe is also visible in the olfactory organ in whole mount (rectangle). (C′) At higher magnification, the *Sof-FMRFa* riboprobe seems to be located within cell bodies (arrowhead) of the olfactory organ. (D) Histamine-LIR staining in the olfactory organ neuropil shows extensions from putative cell bodies (arrows) toward the surface of the olfactory epithelium, which terminate in brightly labeled punctata (arrowheads). The inset shows anti-histamine (red) double-labeled with anti-AcTub (green). There is no colocalization between tubulin-LIR cilia and histamine-LIR cell bodies (arrows) or the punctata (arrowheads) at high magnification. (E) Immunohistochemistry of the olfactory organ in whole mount reveals small, round, tubulin-rich structures (green) underneath the surface of the olfactory epithelium and a few putative synaptic structures labeled with anti-NOS (red, arrowheads). (F) Staining an embryo at stage 27 revealed no APGWa-LIR staining in the olfactory organ, although some putative cell bodies were present near the edge of the optic lobe (arrowhead). (G) Serotonin immunohistochemistry in the olfactory organ of a stage 27 embryo shows neuropil that extends along the basal edge of the olfactory organ. (H) The olfactory nerve, which is also 5-HT-LIR, projects from the neuropil. 5-HT, serotonin; AcTub, acetylated α-tubulin; APGWa, APGWamide; FMRFa, FMRFamide; HA, histamine; NOS, nitric oxide synthase; Olf O, olfactory organ; Olf N, olfactory nerve. *Sof-FMRFa, Sepia officinalis*-FMRFamide. Scale bars: A, B, D, E−H = 100 μm; A inset = 50 μm; C, C′ = 500 μm; D inset = 50 μm.



DOI: 10.1021/acschemneuro.8b00021
ACS Chem. Neurosci. 2018, 9, 2074−2088

positive (not shown), as were somata and fibers in the olfactory lobe (see below). Because of this absence of APGWa-LIR staining in the Olf O, this peptide appears to be disqualified as a possible neurotransmitter used by OSNs in early development. However, APGWa-LIR cell bodies have been previously described in the Olf E of adult *O. vulgaris*.[40]

*Serotonin.* Our work also suggests that 5-HT may play a role in efferent control. 5-HT has previously been associated with the cephalopod olfactory system.[68,55,40] For instance, it first appears in the developing olfactory lobes of the pygmy squid *Idiosepius notoides* around stage 24.[69] Our results demonstrate that 5-HT-containing fibers were abundant in the olfactory nerve and in a layer of neuropil lying at the base of the Olf O, but not within the Olf E itself nor in any cell bodies in the Olf O (Figure 4G, H). As with the transmitters mentioned above, the distribution of 5-HT is reminiscent of staining patterns previously described in gastropods. 5-HT has been described in the rhinophores of *Aplysia*[24,18] and *Phestilla*[21] but is isolated to processes and ganglionic neuropil and is not found in the peripheral sensory cell bodies, a finding which is consistent with the staining pattern seen here in the Olf O of *S. officinalis*. This suggests 5-HT in cephalopods may efferently control the cell bodies of the Olf O. Moroz et al.[70] noted a similar pattern in the sea slug *Pleurobranchaea,* and also suggested that it might play a role in efferent control of sensory pathways in gastropods.

**The Olfactory Nerve.** The olfactory nerve was visible using anti-FMRFa, anti-5-HT, anti-HA, and anti-AcTub by stage 25. The diameter of the olfactory nerve at stage 25 (15 ± 4 $\mu$m; $n$ = 4) is smaller than at stage 30 (20 ± 3 $\mu$m; $n$ = 4). A crystal of DiI, placed directly on the Olf O for approximately 24 h, resulted in the dye permeating into the olfactory nerve over the course of several months, and allowed for mapping of the pathway of the olfactory nerve as it projected to the olfactory lobe (Figure 5A, red). The olfactory nerve projected from the basal neuropil of the Olf O (Figure 5B) and bent around the posterior curve of the optic lobe (Figure 5C, D). The nerve next curved around the ventral optic lobe (Figure 5D) and then changed direction and projected dorsally, between the optic lobe and supraesophageal mass (Figure 5E). Once it reached the olfactory lobe, the labeled fibers fanned into multiple faint, small branching projections that were hard to visualize (Figure 5E). However, there were brightly stained cell bodies in and surrounding the olfactory lobe.

**The Olfactory Lobe Development and Morphology.** As early as stage 14, cells cluster to form the beginnings of the optic, cerebral, visceral, and pedal ganglia and begin to differentiate by stage 21.[71,52] The beginnings of the olfactory lobe appear in stage 23 as a swelling between the supra-esophageal mass and the optic lobe anlagen.[57] We determined the size and organization of the developing olfactory lobe based upon a combination of staining with riboprobes for *Sof-Syt*, anti-AcTub, and phalloidin. By stage 25 the olfactory lobe was comprised of loosely organized neuropil, and averaged 107 $\mu$m across (left to right) and 160 $\mu$m in length (along the dorsal-ventral axis; not shown; $n$ = 3).

The overall shape of the olfactory lobe was in place by stage 27 and did not change through subsequent development. As an extension of the optic tract, the lobe had a substantial thickness (along the anterior-posterior axis) and was easily recognizable as a collection of three lobules (posterior, medial, and anterior, or also known as lobules 1, 2, and 3, respectively; Figure 6A). The lobules were offset in such a way that, in posterior sections,

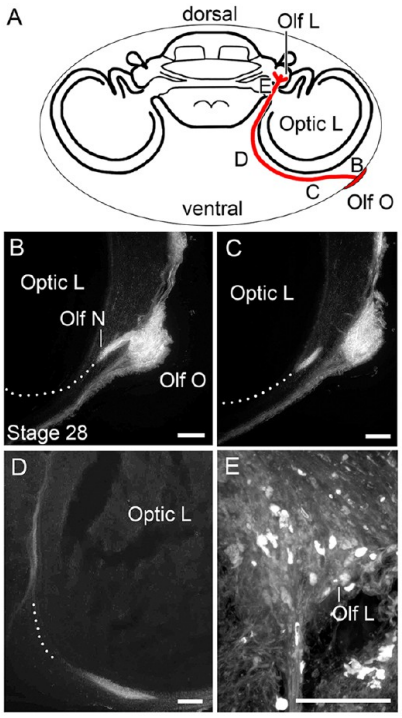


**Figure 5.** Olfactory organ and nerve stained with DiI. (A) Diagrammatic representation of a transverse section through the brain demonstrating locations of the olfactory organ, lobe, and nerve (red). (B) Olfactory organ in a stage 28 embryo is brightly labeled and the olfactory nerve can be seen projecting from its base. The dotted lines help visualize the pathway of the olfactory nerve which cannot be seen in individual sections. (C) The next section of olfactory nerve can be seen further away from the olfactory organ as it follows the ventral and posterior curve of the optic lobe. (D) The olfactory nerve curves around the optic lobe toward the dorsal side once it reaches the medial side. It then projects in an anterior direction between the optic lobe and supraesophageal mass. (E) The nerve innervates the anterior end of the olfactory lobe where it then branches into smaller bundles of fibers, potentially terminating on what appear to be brightly labeled cell bodies. Olf L, olfactory lobe; Olf N, olfactory nerve; Olf O, olfactory organ; Optic L, optic lobe. Scale bars represent approximately 100 $\mu$m.

both lobule 1 and 2 were visible in the same 30 $\mu$m section, and, in more anterior sections, lobules 2 and 3 were visible together (Figure 6A). The olfactory lobe was widest on its dorsal end and narrowed toward the ventral end, thus forming a triangular shape (Figure 6B). In addition, the lobe tapered at its anterior and posterior ends, so that the narrowest regions of neuropil were in the far anterior end (lobule 3) and the widest regions were in the middle of the lobe. The individual lobules were each formed by a central neuropil core surrounded by neurons. Lobule 3 was comprised primarily of neuropil with fewer cell bodies than lobules 1 or 2 because it is the most interwoven with the optic tract.

The size of the olfactory lobe increased from stage 27 through hatching in all dimensions. In late stage embryos (stage 27–29), the neuropil averaged 255 ± 87 $\mu$m ($n$ = 15) in length (dorsal-ventral axis) and 89 ± 49 $\mu$m ($n$ = 15) in width (left to right; Figure 6C1–E3). The bundles of fibers and surrounding neurons also increased in number throughout development until the lobe reached a dense composition of indistinguishable fibers at hatching.


DOI: 10.1021/acschemneuro.8b00021
ACS Chem. Neurosci. 2018, 9, 2074–2088

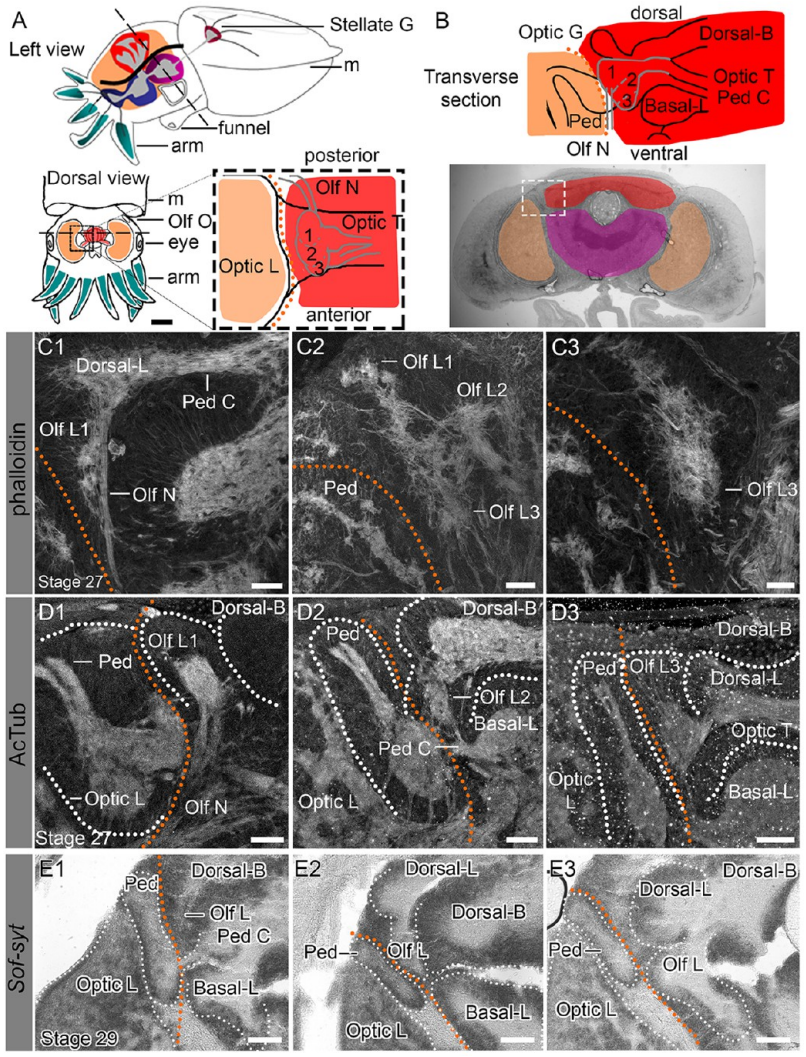


**Figure 6.** Staining by phalloidin, anti-AcTub, and *Sof-Syt* riboprobe in the central nervous system of *S. officinalis*. (A) The diagram represents an embryonic cuttlefish in profile (left side) and head-on (dorsal) including the mantle, olfactory organ, eye, arms, and brain. Inside the rectangle is a diagrammatic depiction of the left olfactory lobe positioned along the optic tract from the dorsal perspective. Orange shading denotes the optic lobe region including the peduncle lobe; red shading denotes the supraesophageal mass region; the dotted orange line denotes the border between the two. (B) Diagram which represents the olfactory lobe in transverse sections (as if the embryo were cut parallel to the orientation of the dotted lines in (A); dorsal up, ventral down; and in the same orientation as Figure 5A) as the panels are oriented in (C1−E3). The purple shading denotes the subesophageal mass region. (C1−C3) Phalloidin labels F-actin in the optic, peduncle, dorsal-lateral, and olfactory lobes in a stage 27 embryo. (C1) The olfactory nerve enters the ventral end of olfactory lobule 1 which also connects to the dorsal-lateral and peduncle commissure. (C2) In a more anterior section, the olfactory lobe has a stereotypical triangular shape with a wider dorsal end. (C3) An anterior section of olfactory lobule 3 has a narrow diameter due to integration with the optic tract. (D1−D3) Anti-AcTub staining in a section through the olfactory and surrounding lobes in a stage 27 embryo. (D1) The optic, peduncle, and olfactory lobes contain AcTub-postitive neuropil. (D2) Olfactory lobule 2 is connected to the peduncle lobe and basal-lateral lobe via the peduncle commissure. (D3) A more anterior section shows connectivity between olfactory lobule 2 and dorsal-lateral lobe. (E1−E3) The olfactory lobe and surrounding central nervous system is visualized with the *Sof-Syt* riboprobe in a stage 29 embryo. (E1) The peduncle lobe in a posterior section connects to the basal-lateral lobe via the peduncle commissure. (E2) The olfactory lobe is more clearly visible in a more anterior section as an extension of the dorsal-lateral lobe. (E3) Lobules 2 and 3 connect to the dorsal-basal lobe through the optic commissure. AcTub, acetylated $\alpha$-tubulin; Basal-L, basal-lateral lobe; Dorsal-B, dorsal-basal lobe; Dorsal-L, dorsal-lateral lobe; m, mantle; Olf L1, olfactory lobule 1; Olf L2, olfactory lobule 2; Olf L3, olfactory lobule 3; Olf N, olfactory nerve; Olf O, olfactory organ; Optic G, optic gland; Optic L, optic lobe; Optic T, optic tract; Optic L, optic lobe; Ped C, peduncle commissure; Ped, peduncle lobe; *Sof-Syt*, *Sepia officinalis*-synaptotagmin riboprobe; Stellate G, stellate ganglion. Scale bars: 100 $\mu$m.

Phalloidin has often been used in studies of developing molluscan musculature,[50] but it also labels F-actin in the cephalopod central nervous system.[48] Phalloidin has also been described as a consistent marker used to visualize glomeruli in a wide variety of species, since glomeruli have a much higher intensity of phalloidin staining than the surrounding regions.[51] The staining pattern rendered by phalloidin was also analyzed in the cuttlefish central nervous system in the vicinity of the olfactory lobe (Figure 6C1−C3, stage 27). F-actin was brightly labeled in the neuropil of the dorsal-lateral and olfactory lobes and in the peduncle commissure, with labeling in the olfactory nerve as well (Figure 6C1). The neuropil seemed to have some general directionality, particularly along narrow tracts such as the peduncle commissure and optic tract, although bundles of axons often crossed each other at different angles. This observation was less true for the neuropil at the center of the


DOI: 10.1021/acschemneuro.8b00021
ACS Chem. Neurosci. 2018, 9, 2074−2088

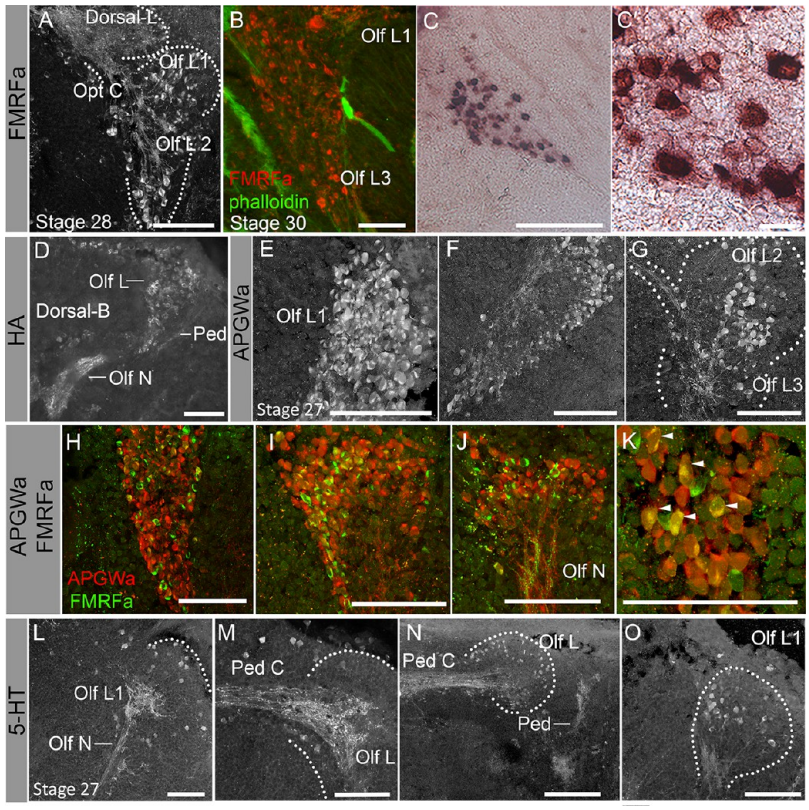


**Figure 7.** Neurotransmitters in the olfactory lobe. (A) FMRFa-LIR staining in a section through the middle of the olfactory lobe in a stage 28 embryo. Cell bodies are visible in olfactory lobules 1 and 2. (B) Posterior section of a stage 30 olfactory lobule 1 double-labeled with anti-FMRFa (red) and phalloidin (green) to show that the cortex of cell bodies surrounding the lobule is almost completely devoid of neuropil, which is restricted to the lobule core. (C) High magnification of the *Sof-FMRFa* expression in the left olfactory lobe in a stage 27 embryo is visualized with ISH. (C′) Higher magnification of (C) demonstrates *Sof-FMRFa* expression inside the cell bodies of the olfactory lobe. (D) Histamine immunoreactive staining in the central nervous system of a stage 28 embryo shows possible cell bodies in the olfactory lobe (lobule 1) with almost no visible neuropil. The olfactory nerve projects toward the anterior end of the lobule. Light staining is also apparent in the peduncle lobe. (E) Anti-APGWa staining is present in the olfactory lobe of a stage 27 embryo. The posterior surface of olfactory lobule 1 is a cortex of APGWa-positive cell bodies. (F) In a more anterior section, neurons wrap around the outside of the lobe while the interior neuropil is visible. (G) The anterior-most section contains neurons of olfactory lobule 2 and neuropil of lobule 3. (H) Anti-APGWa (red) and anti-FMRFa (green) double-labeling in the olfactory lobe in a stage 27 embryo shows that the surface cortex of olfactory lobule 1 is primarily composed labeled cell bodies. A few cell bodies are colabeled (yellow). (I) Olfactory lobule 1 has more of the central neuropil exposed, more FMRFa-LIR neurons in the anterior of the lobule, and more cell bodies that are colabeled in a more anterior section. (J) The olfactory nerve, projecting to the anterior tip of olfactory lobule 1, contains both APGWa-positive and FMRFa-positive fibers with no colocalization. (K) High magnification of the posterior cell body cortex of lobule 1 shows individual cell bodies in the olfactory lobe; colabeled (yellow) cell bodies are identified with arrowheads. (L) 5-HT-LIR staining in the olfactory lobe and surrounding central nervous system in a posterior section of a stage 27 embryo demonstrates how the olfactory nerve innervates olfactory lobule 1 neuropil, with neurons around the periphery of the lobule. (M) The peduncle commissure connects the dorsal end of the olfactory lobule 1 neuropil to the dorsal-basal lobe. (N) 5-HT-LIR cell bodies surround the central neuropil of the olfactory lobe. The peduncle lobe also contains 5-HT-LIR neuropil. (O) High magnification showing the 5-HT-LIR staining in neurons and neuropil of olfactory lobule 1. 5-HT, serotonin; Dorsal-B, dorsal-basal lobe; Dorsal-L, dorsal-lateral lobe; Olf L1, olfactory lobule 1; Olf L2, olfactory lobule 2; Olf L3, olfactory lobule 3; Olf N, olfactory nerve; Optic C, optic commissure; Ped, peduncle lobe; Ped C, peduncle commissure. Scale bars: 100 $\mu$m except C′ = 10 $\mu$m.

lobes, in which bundles of fibers seemed to project at all angles without any organization (Figure 6C2, C3). At no point in the examined stages were spheroidal clusters of F-actin staining, indicative of olfactory glomeruli, apparent in the olfactory lobe or anywhere else in nearby regions of the brain.

Anti-AcTub stained the neuropil of the central nervous system in the dorsal-basal lobe, olfactory lobe, optic lobe, and peduncle lobe (Figure 6D1). At stage 27, AcTub-LIR staining filled the lobes as a condensed conglomeration of fluorescence, although upon close inspection individual bundles of fibers and structures were apparent, particularly extending off and in-between individual lobes. These long projections extended from one neuropil to another: for example, in the peduncle commissure between the olfactory lobe and the peduncle lobe (Figure 6D2) and in the optic tract, between the dorsal-lateral and olfactory lobe (Figure 6D3).

*Sof-Syt* riboprobe was localized to the cell bodies on the periphery of the lobes in the central nervous system. The intensely labeled cell body cortex delineated the edges between individual lobes while the neuropil cores were lightly labeled, which demonstrated that the majority of the lobes in the cuttlefish brain were filled with neuropil and had an outer cortex of cell bodies (Figure 6E1–E3, stage 29). This staining assisted in visualizing the individual lobes of the brain.

In week-old hatchlings, the olfactory lobe had not changed in structure, shape, or organization, but had increased greatly in size from stage 29. The average size of the total lobe length


DOI: 10.1021/acschemneuro.8b00021
ACS Chem. Neurosci. 2018, 9, 2074−2088

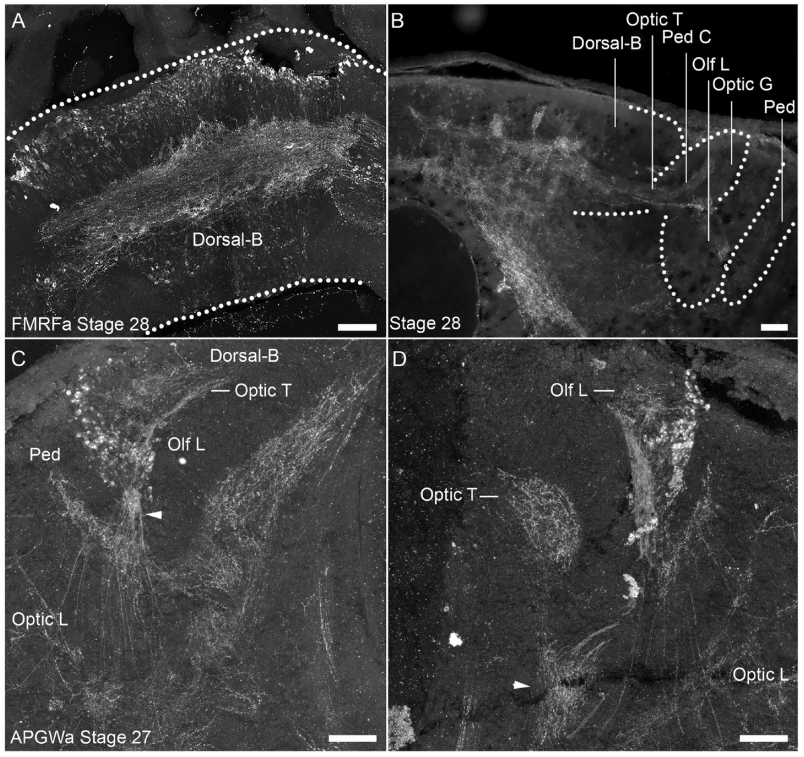


**Figure 8.** Interconnectivity of the olfactory lobe. (A) FMRFa-LIR staining is present in the supraesophageal mass at stage 28. Cell bodies on the dorsal edge project neurites anteriorly into the central neuropil of the dorsal-basal lobe. Many of the horizontal fiber bundles in the neuropil project into the optic tract, some of which innervate the olfactory lobe. (B) Anti-FMRFa staining in the dorsal-basal lobe connects via the optic tract to the optic gland, olfactory lobe, and peduncle lobe. (C) APGWa-LIR staining also labels the interconnectivity of the olfactory lobe to other lobes in the central nervous system including the peduncle, optic, and dorsal-basal lobes through the optic tract. The arrowhead indicates a collection of fibers near the point of termination of the olfactory nerve onto the olfactory lobe. (D) In a more posterior section, the neuropil of the optic tract is only partly visible, along with projections from the olfactory lobe toward the subesophageal mass. Dorsal-B, dorsal-basal lobe; Olf L, olfactory lobe; Optic G, optic gland; Optic L, optic lobe; Optic T, optic tract; Ped, peduncle lobe; Ped C, peduncle commissure. Scale bars: 100 $\mu$m.

(dorsal-ventral) was 528 ± 67 $\mu$m ($n$ = 15) and mean lobe width (left to right) was 213 ± 78 $\mu$m ($n$ = 15).

Thus, phalloidin, anti-AcTub, and *Sof-Syt* riboprobes did not show any signs of glomeruli in cuttlefish, nor did distribution patterns of neurotransmitters in the olfactory lobe reveal glomeruli in the present study (see below) or in previous work in *Octopus*,[38−40] but they did provide further information about the organization of the olfactory system.

**Neurotransmitters in the Olfactory Lobes.** *FMRFamide-Related Peptides.* FMRFa-LIR staining was visible in cell bodies of olfactory lobules 1, 2, and 3 surrounding a central neuropil that connected to the optic commissure (Figure 7A, B), although immunoreactive somata were more prevalent in lobules 1 and 2 than in lobule 3 (not shown). This centralized neuropil, in addition to containing FMRFa-LIR fibers, also contained F-actin (Figure 7B). A *Sof-FMRFa* riboprobe confirmed the presence of a large quantity of neurons that expressed FaRPs in olfactory lobule 1 (mean diameter 10 $\mu$m; $n$ = 45; Figure 7C, C′). The general shape of olfactory lobe was also apparent, with most of the neurons located dorsally as the lobe tapered to a narrow point on the ventral end.

The presence of both IHC and ISH staining in the lobe suggests that in addition to FaRPs being a neurotransmitter in OSNs, there are also second order neurons within the olfactory lobe that are FMRFa-positive. Intense FMRFa-LIR staining was also present in the rest of the brain, including cell bodies and a centralized neuropil in the dorsal-basal lobe. There were also connections between the dorsal-basal lobe, olfactory lobe, optic gland, and peduncle lobe through the FMRFa-positive fibers in the optic tract and peduncle commissure (Figure 8A, B).

*Histamine.* The triangular shape of the olfactory lobe was easily observed with IHC using anti-HA ($n$ = 16; stage 27; Figure 7D). Numerous cell bodies with mean diameters of 10 ± 2 $\mu$m ($n$ = 13) were distributed around the olfactory lobe. While there was no staining in the neuropil of the olfactory lobe, there was dim neuropil staining in the peduncle lobe, as well as the neuropil and cell bodies on the dorsal edge of the dorsal-basal lobe. There were no systematic differences in immunoreactivity between the lobes. HA-LIR axons in the olfactory nerve were also seen entering the ventral end of the olfactory lobe, consistent with our evidence that HA is a neurotransmitter in cuttlefish OSNs.

*APGWamide.* Several neuropeptides involved in reproduction, including FaRPs, neuropeptide Y, gonadotropin-releasing hormone, and APGWa, were reported in the OSNs and fibers of the *O. vulgaris* olfactory lobe.[39,40] The abundance of reproductive peptides in the olfactory system in *Octopus* suggested APGWa might also be a useful marker to help describe the organization of the olfactory lobe in *Sepia*.

Despite the lack of APGWa in the Olf O (see above), immunoreactive neurons were abundant throughout the olfactory lobe with no noticeable difference between lobules (Figure 7E−G). APGWa was also present in the rest of the central nervous system, particularly in the neuropil of the optic lobe, peduncle lobe, optic tract, and dorsal-basal lobe (Figure


DOI: 10.1021/acschemneuro.8b00021
ACS Chem. Neurosci. 2018, 9, 2074−2088

8C, D). The staining also projected to the subesophageal mass and the optic lobe (Figure 8D).

Double-labeling experiments with anti-FMRFa and anti-APGWa showed that on the posterior surface of olfactory lobule 1, 66% ($n \sim 50$ neurons) of the neurons were APGWa-positive, 26% ($n \sim 25$) were FMRFa-positive, and 8% ($n \sim 6$) were colocalized (Figure 7H−K). Although no colabeling was apparent in the nerve, several cell bodies in the dorsal end of lobule 1 were colabeled (Figure 7K, arrowheads). In other molluscs, such as the land snail *Cornu aspersa*, FaRPs and APGWa have been shown to act synergistically, and were often coexpressed in the same neurons controlling male copulation.[72]

*Serotonin.* 5-HT has been previously described in the olfactory system of cephalopods;[68,55,65] however, we found additional anti-5-HT staining in the neuropil of the olfactory lobe consistent with a previous study of 5-HT in the adult squid *I. notoides*.[69] Here, we observed that 5-HT-LIR staining was present in both neurons and neuropil throughout the central nervous system of *S. officinalis,* including neurons in the optic and dorsal-basal lobe and fibers of the peduncle lobe and olfactory nerve (Figure 7L). The 5-HT-LIR staining of the olfactory nerve innervating lobule 1 confirmed similar fainter staining observed with DiI stain (Figure 5E). The neuropil in the anterior region of the olfactory lobe was 5-HT-positive with a few cell bodies around the periphery of lobule 2 (Figure 7M, N). When lobule 1 was viewed at a higher magnification, neurons could be observed to project their axons to a central core of neuropil (Figure 7O).

Despite the loose disorganization of the lobe at stage 25, it appears to be functional based on behavioral evidence previously published.[56,47,57] As the embryo develops, the Olf O and olfactory lobe both continuously grow, and most likely continue to do so well into adulthood.[54] As the Olf O increases in surface area and number of OSNs, the olfactory lobe may also increase its area to accommodate a proliferation of incoming fibers. In addition to overall growth, the olfactory lobe also increases in refinement and organization throughout development, from a loose collection of fibers to a tightly packed centralized neuropil. The implications of this rudimentary functionality at early developmental stages and the increase in size and complexity of the lobe throughout development are, however, presently unknown.

## SUMMARY AND EVOLUTIONARY PERSPECTIVES

Taken together, the various histological stains which we employed in the present study provide an initial, but nonetheless detailed, description of the organization and development of the olfactory system of the cuttlefish, *S. officinalis*. We provide evidence for multiple cell types of OSNs as well as the neurotransmitters in the organ and nerve. We also describe the organization of the olfactory lobe and identify possible afferent and efferent neurotransmitters to and from the lobe (Figures 8 and 9). Finally, we explored the lobe for potential glomerular structures and did not find anything resembling those described in gastropods, vertebrates, or arthropods. Not only do these insights help us understand how cephalopods detect, process, and organize olfactory inputs, these descriptions can also be used to draw inferences about the evolution of olfaction, as related particularly to the involvement of glomeruli in initial stages of processing olfactory information.

There are several key similarities between the olfactory glomeruli of different phyla (reviewed in ref 10) that we use as morphological criteria to identify a potential glomerulus in

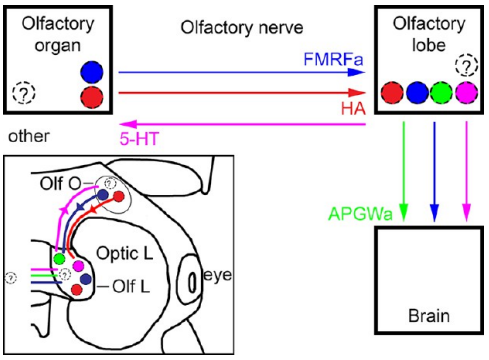


**Figure 9.** Neurotransmitters in olfactory pathways and putative sensory neurons. Schematic that represents the suggested locations of different neurotransmitter-like immunoreactivity presented in this study. In the olfactory organ, FMRFa (blue) and histamine (red) are suggested to be neurotransmitters of the olfactory sensory neurons that project to the olfactory lobe. In the olfactory lobe, 5-HT-positive cell bodies (magenta) are possible efferent neurons that project to the olfactory organ. APGWa (green), FMRFa, and 5-HT also project to other lobes of the brain. 5-HT, serotonin; APGWa, APGWamide; FMRFa, FMRFamide; HA, histamine; Olf L, olfactory lobe; Olf O, olfactory organ; Optic L, optic lobe.

cuttlefish. First, all glomeruli described thus far, except for those in gastropods (see above), have been found in the central nervous system, i.e., in the olfactory bulb in vertebrates, the olfactory lobe in crustaceans, and the antennal lobe of insects. Second, previously described glomeruli have an overall spherical shape, as also seen in vertebrates, crustaceans, and insects. Third, glial cells surrounded glomeruli in all animal groups, most likely isolating individual glomeruli from each other to define their sharp outlines. Fourth, glomeruli seem to be generally similar in size, within the range 40−100 $\mu$m.[19] Fifth, glomeruli across the animal kingdom are marked by a high turnover of neurons.[73,51] Since F-actin is plentiful in newly developed neurites, phalloidin stains glomeruli in many animals.[51,74] In this present study, we applied these criteria and suggest that *Sepia*, like *Nautilus* and *Octopus*,[10] may not have structures resembling classical glomeruli in their olfactory lobes. Final confirmation of this hypothesis will come from wider surveys of related brain structures which might process olfactory information and perhaps the use of glial markers.

A question might arise regarding whether suckers and sucker ganglia should be considered as part of the olfactory pathway. We argue that while ganglia have been widely observed at the base of suckers, we do not believe that these structures serve the same purpose as olfactory glomeruli. Suckers are generally considered to be contact chemosensory organs as mentioned above. Additionally, those ganglia would be points of convergence for all neurons in the sucker, regardless of chemical quality or even sensory modality. Alternatively, olfactory glomeruli are points of convergence based on olfactory receptor type (therefore indicating chemical quality) and not location.

One explanation for why glomeruli would have been previously described in gastropods but not cephalopods could be that glomeruli do exist in certain molluscs (i.e., some gastropods) but have been lost in the cephalopods. In fact, glomeruli appear to have been independently lost several other times in animal evolution. For example, modern toothed whales have completely lost their glomeruli, along with their entire sense of olfaction,[75] as have some arthropods.[76] Recent studies


DOI: 10.1021/acschemneuro.8b00021
ACS Chem. Neurosci. 2018, 9, 2074−2088

have suggested that cephalopods differ greatly from other molluscs in their ability to edit RNA, a quality that allows them to diversify their transcriptome at the expense of genetic evolution.[77] Perhaps this specialized process has resulted in an alternative olfactory organization without the use of glomeruli, despite their molluscan ancestry.

It seems to be more likely, however, that olfactory glomeruli may not exist in any molluscs, at least not in the same sense that they have been described in arthropods and vertebrates. Glomeruli were first suggested to be present in a gastropod species before molecular studies were designed to define glomeruli in vertebrates and arthropods.[19] The peripheral locations of gastropod glomeruli differ profoundly from their central locations in other animals, but their locations in gastropods also challenge explanations of how these structures might serve as foci for the convergence of afferent inputs from across the Olf E as has previously been described in other species.[11,10,15] In addition, there are relatively fewer glomeruli in gastropods (20−36 glomeruli depending upon the species) than in vertebrates or arthropods (on the order of 1000−5000 glomeruli in mammals; 50−300 glomeruli in arthropods).[19,11,18] Perhaps most importantly, no evidence yet exists in any molluscs indicating that afferent inputs from OSNs sharing specific receptor proteins segregate to innervate target glomeruli according to the "one receptor, one glomerulus" rule, which is fundamental to our modern understanding of olfactory processing in vertebrates and arthropods.[78] Cummins and Wyeth[18] noted these distinctions and prompted for more molecular studies to further define the gastropod olfactory glomerulus.

Such differences between glomeruli in gastropods and those found in other animals, in combination with a distinct lack of evidence for olfactory glomeruli in cephalopods, suggest that these structures are not found universally among all cephalized animals. With olfactory glomeruli hypothetically isolated to vertebrates and arthropods, it is possible that these structures independently evolved twice to overcome common problems in the processing of sensory information regarding wide arrays of dilute chemicals in these two clades. If true, the question then would remain as to how cephalopods, or in fact any molluscs, organize their olfactory input without glomeruli. Further behavioral and physiological studies in cephalopod olfaction are therefore needed. By understanding the mechanisms by which cephalopods, particularly coleoids, can detect and discriminate odorants, we can better understand the evolution of olfaction across a diversity of animal models.

## METHODS

**Animal Collection.** Eggs from *Sepia officinalis* were gathered near Concarneau, France, in the late springs of 2014−2016 and were subsequently maintained at approximately 20 °C in aerated seawater. Each day, the capsule and chorion layers were removed from several specimens to obtain a collection of developmental stages.[79,80] Under these conditions, embryos generally developed over 30 days (approximately 1 stage/day) and were allowed to develop until just prior to hatching. Embryos from three distinct points in development, mid-stage (stage 25), late-stage (stage 27−29), and immediately before hatching (approximately stage 30), were used to describe the development of the olfactory system. In addition, some hatchlings reared in the Aquatron Facility at Dalhousie University were collected at approximately 1 week old.

All specimens used for experimentation were anesthetized in 7% magnesium chloride in distilled water ($dH_20$) for 20−40 min, until they became unresponsive to stimuli, and then immersed in fixatives. For those embryos reserved for ISH experiments, embryos were opened in RNase-free conditions before anesthetization and fixation. All animal procedures were in compliance with the guidelines of the European Union (Directive 86/609) and the French law (Decree 87/848) regulating animal experimentation, as well as the Dalhousie University Committee on Laboratory Animals protocol (in compliance with the guidelines on procurement of animals used in science published by the Canadian Council on Animal Care). Efforts were made to minimize animal suffering and to reduce the number of animals used.

**Fixation and Tissue Preparation.** After anesthetization, embryos collected for IHC and ISH experiments were decapitated and split in half before fixation. Two different fixatives were used. Paraformaldehyde (PFA) fixative was prepared using 16% PFA (PFA; RT-15710, Electron Microscopy Sciences, Hatfield, PA), which was further diluted to 4% in phosphate buffered saline (PBS; 50 mM $Na_2HPO_4$, 140 mM NaCl, pH 7.2) in which embryos were incubated for 24−36 h. Embryos destined for anti-HA IHC were first fixed in a solution of 2% EDAC (1-ethyl-3(3-dimethylaminopropyl)-carbodiimide; Sigma-Aldrich, Mississauga, ON, Canada) and 0.4% *N*-hydroxysuccinimide in PBS[81] for 24−36 h before postfixing in 4% PFA for an additional 48 h. All fixations occurred at 4 °C with gentle agitation on a shaker, after which embryos were washed in fresh PBS for 12 h before storage in PBS with 0.005% sodium azide at 4 °C or in RNase-free 50/50 glycerol/PBS at 20 °C for embryos reserved for ISH.

**Immunohistochemistry.** Staining protocols described by Croll[82] were used with modifications. Specimens were prepared with either a single- or double-label with one or two primary and secondary antibodies (see below) from different hosts so that they were viewable in different fluorescent channels and/or in combination with phalloidin (see below). Embryos were either processed as halved-heads or as cryosections.

For whole-mounts, pieces of tissue were placed into individual 1.5 or 2.0 mL Eppendorf vials and then incubated in PBS-Tx blocking/diluent solution comprised of PBS with 2% dimethyl sulfoxide (DMSO), 1% Triton X-100, 0.1% bovine serum albumin, and 0.1% normal goat serum (all from Sigma-Aldrich) for 24 h at 4 °C. The blocking solution was then replaced with a solution containing primary antibodies (combined in double labeling experiments) and diluted 1:200 in PBS-Tx. After 10 days at 4 °C, the preparations were rinsed with PBS and agitated at room temperature for 10 min before being rinsed again for four additional times at 10 min intervals. They were then incubated in 1:200 dilutions of fluorescently labeled secondary antibodies in PBS-Tx for an additional 10 days at 4 °C. Specimens were rinsed with PBS using the same procedure used after incubation in the primary antibody. The clearing agent CUBIC (clear, unobstructed brain/body imaging cocktail; 25% Quadrol [(ethylenedinitrilo)tetra-2-propanol], 25% urea, 15% Triton X-100 (all % calculated as weight/volume) in $dH_2O$[83]) was used to improve visualization in whole-mount specimen.

For IHC on sections, fixed embryos were placed in a phosphate saccharose buffer (12% saccharose in 120 mM phosphate buffer, pH 7.2) for 24 h, after which the solution was exchanged with fresh buffer for another 24 h. Next, embryos were incubated in gelatin/saccharose phosphate buffer (120 mM phosphate buffer, 12% saccharose, and 7.5% gelatin) for 1 h, or embedded in Fisher HealthCare Tissue-Plus O.C.T. (optimal cutting temperature) compound (ThermoFisher Scientific, Waltham, MA) or Tissue-Tek O.C.T. compound (Sakura Finetek USA Inc., Torrance, CA) and then rapidly frozen at −80 °C. Blocks were subsequently cut into 30−60 μm sections along the transverse (i.e., horizontal or axial) plane using a cryostat (CM1510; Leica Microsystems GmbH, Wetzlar, Germany) and placed on either SupraFrost Ultra or SuperFrost Ultra Plus Adhesion (ThermoFisher Scientific) slides, previously coated with 0.5% gelatin and 0.05% chromium potassium sulfate dodecahydrate ($CrK(SO_4)_2$; R&D Systems Protocol; https://www.rndsystems.com/resources/protocols/protocol-preparation-gelatin-coated-slides-histological-tissue-sections).

Individual slices were isolated from one another on each slide with a hydrophobic pen (Liquid Blocker Pap Pen for Immunostaining,


DOI: 10.1021/acschemneuro.8b00021
ACS Chem. Neurosci. 2018, 9, 2074−2088

Sigma-Aldrich) to avoid solution dispersal. Slides were incubated under the same conditions as in whole-mount, except that they were placed in a sealed humid chamber with a moist paper towel to avoid dehydration. Incubations in the primary and secondary antibodies only lasted 24 h each with three gentle washes over half hour periods between incubations and before mounting. Sections were then mounted in a medium of 6 g of glycerol, 2.4 g of MOWIOL (EMD Milipore, Billerica, MA), 6 mL of $dH_2O$, and 12 mL of 0.2 M Tris buffer, pH 8.5) for viewing.

Some slides were alternatively processed using secondary antibodies that were coupled with biotin rather than fluorescent markers. After antibody incubation, the slides were transferred to an avidin−biotin−HRP complex for 1 h (ThermoFisher Scientific, Waltham, MA). These specimens were processed for DAB (3, 3′-diaminobenzidine) staining using the VECTASTAIN Elite ABC kit (Vector Laboratories, Burlingame, CA) according to instructions. Finally, slides were washed in the same conditions as fluorescent IHC and mounted in MOWIOL.

**Primary and Secondary Antibodies.** Most antibodies used in this study were obtained commercially so the specificity and affinity to their respective antigens have been systematically demonstrated over several different conditions and in a variety of vertebrate and invertebrate species, as described by the suppliers. Antibodies were incubated with tissue in PBS at dilution 1:200. AcTub, a post translational modification of an $\alpha$-tubulin that increases microtubule stability,[84] was labeled using clone 6-11B-1 (monoclonal mouse T6793, Sigma-Aldrich). This clone, raised against sea urchin tubulin, has been shown to reliably stain neurons in a variety of invertebrates, including molluscs.[35,85,47,48,57,49,42] Likewise, anti-universal nitric oxide synthase (uNOS; polyclonal rabbit; Affinity Bioreagents, Golden, CO, PA1-039) antibody has also been used reliably in a variety of molluscan studies.[62,38,46,86] The HA antibody has been extensively published, and reactivity has been demonstrated in vertebrates (*Mus musculus*[87]), arthropods (*Drosophila*[88]), and molluscs.[64,46,65,89] Labeling with the FMRFa antibody (polyclonal rabbit Immunostar Inc., Hudson, WI, 20091, lot #1331002) has been described in multiple phyla, including Mollusca.[66,67,53,61,90,55,54] The 5-HT antibody (polyclonal rabbit, #20080, Immunostar, Hudson, WI) has been used extensively in studies in diverse phyla,[13,14] including Mollusca.[68,24,55,69,46,18,40] Finally, the antibody against APGWa was raised for a study in the snail, *Lymnaea stagnalis*, and was conducted in conjunction with ISH to confirm its specificity.[91] Since then, the antibody has been used to label neurons and neuropil containing APGWa in a variety of molluscs including *Aplysia spp.*, *Placopecten magellanicus*, and *Octopus vuglaris*.[92,93,38,40]

Fluorescent detection of immunoreactive staining included the following secondary antibodies: goat anti-mouse Alexa Fluor 488, cat #A28175 from Invitrogen (Carlsbad, CA); donkey anti-mouse Alexa Fluor 555, cat #A31572 from Invitrogen; donkey anti-rabbit Alexa Fluor 488, cat #A21206 from Invitrogen; goat anti-rabbit Alexa Fluor 555, cat #A21428 from Invitrogen; goat anti-guinea pig Alexa Fluor 555, cat #A21428 from ThermoFisher. Nonfluorescent detection of immunoreactive staining employed a goat anti-rabbit antibody conjugated to biotin, CAT #BA-1000 from Vector Laboratories.

**Controls.** Consistent staining patterns were observed using different fluorophores (Alexa Fluor 488 vs Alexa Fluor 555) and when comparing fluorescent vs nonfluorescent secondary antibodies. Omission controls were conducted as tissues were tested for background autofluorescence in the absence of any antibodies. Fixed tissue showed no autofluorescence. In addition, sections processed without primary antibody incubation confirmed that there was no significant, unspecific secondary antibody binding.

**Other Histofluorescent Labeling.** Some specimens were colabeled with phalloidin conjugated to AlexaFluor 488 (Invitrogen, A12379, lot #165101, dilution 1:200), which was applied at the same time as the secondary antibodies.

In additional specimens (stage 28), the fluorescent lipophilic dye, DiI ((2*Z*)-2-[(*E*)-3-(3,3-dimethyl-1-octadecylindol-1-ium-2-yl)prop-2-enylidene]-3,3-dimethyl-1-octadecylindole; perchlorate), was used to trace the nerve from the Olf O to the olfactory lobe. DiI (Molecular Probes, Eugene, OR, D-282, lot #4591-24, Alexa Fluor 555) has been used in a variety of physiological studies to identify the *Xenopus* extrabulbar olfactory pathway,[45] the moth olfactory lobe,[44] and gastropod peripheral sensory cells.[46] Cuttlefish heads that were fixed overnight in 4% PFA were mounted in 10% agarose in PBS in a culture dish well with 0.005% sodium azide. This agarose gel provided a stable base in which the head could be oriented so that the Olf E was exposed. A small crystal of DiI was placed directly on the olfactory pit for 24 h. The heads were then carefully removed from the agarose and the external DiI was rinsed with PBS before the embryonic heads were stored in PBS with 0.005% sodium azide for 8 to 12 months to allow the diffusion of DiI through the olfactory nerve to the brain.

**Gene Isolation and Probe Synthesis.** General procedures for gene isolation, orthology analyses, and primer design for probe synthesis have been previously described.[54,41] The orthology of each of the sequences has been determined using phylogenetic analyses (Mega7 software) and specific primers were designed for polymerase chain reaction (PCR) amplification. Gene fragments were amplified by PCR under the following conditions: 95 °C for 5 min + (95 °C for 30 s, 58 °C for 30 s, 72 °C for 1 min) for 35 cycles +72 °C for 10 min. As templates, we used total RNA of *S. officinalis* extracted from a pool of embryos from stages 15 to 30 using Tri Reagent (MRC, Cincinnati, OH) and an RNA purification kit (Qiagen, Valencia, CA). mRNAs were isolated with the genomic (gDNA) eliminator column and converted into cDNA by the Omniscript reverse-transcriptase (Qiagen). PCR products of the expected size were cloned into TOPO vectors (Invitrogen) and sequenced by GATC Biotech (Konstanz, Germany). RNA probes were generated by in vitro transcription using digoxigenin-11-UTP (DIG RNA labeling mix kit; Roche, Meylan, France). Antisense and sense probes were obtained with T3 or T7 polymerase (Roche) and were purified by cold precipitation with lithium chloride and anhydrous alcohol.[41] Sense RNA probes were used as negative controls.

**In Situ Hybridizations.** Whole-mount ISH was done as previously described in Buresi et al.[41] ISH was also conducted on cryosections prepared in RNase-free conditions. While most of the procedure on cryosections was consistent with that done on whole-mount preparations, any permeability treatments such as the methanol dehydration steps and proteinase K were unnecessary and therefore omitted. After initially rinsing the slides in PBS at room temperature, sections were rinsed again in a saline-sodium citrate buffer (SSC (5×) 0.3 M sodium citrate; 3 M NaCl, pH 8.0). Slides were then incubated in a humid chamber at 65 °C for 2 h in the prehybridization buffer (50% deionized formamide, SSC (5×), 40 $\mu$g/mL salmon sperm DNA, Denhard's solution (5×), and 10% dextran sulfate). The hybridization buffer included an addition of 300 ng/mL of probe to the prehybridization buffer and was left overnight in a humid chamber. After rinses in SSC (2×) and SSC (0.1×) at 65 °C, slides were transitioned to MABT (100 mM maleic acid, 150 mM NaCl, 0.1% Tween-20, pH 7.5) and then incubated for 1 h with the addition of 4% blocking buffer and 15% fetal bovine serum at room temperature. Sections were then incubated in anti-DIG antibody (1:500; Sigma-Aldrich polyclonal sheep #11333089001) conjugated to alkaline phosphatase (AP) and diluted 1:500 in 1% blocking buffer, 5% fetal bovine serum, and 94% MABT at 4 °C for 2 h. Slides were rinsed in MABT and then left at room temperature in MABT overnight. Finally, AP buffer (100 mM Tris-HCl pH 9.5, 100 mM NaCl, 50 mM $MgCl_2$, 0.1% Tween-20, and 1 mM levamisol) was added to the sections for 20 min before revelation with the addition of 150 $\mu$g/mL 5-bromo-4-chloro-3-indolyl phosphate (BCIP) and 300 $\mu$g/mL nitroblue tetrazolium chloride (NBT) until the desired contrast was reached. Slides were then rinsed and mounted in MOWIOL (see above).

**Microscopy.** All fluorescent histology slides were first viewed on a conventional Leica DM 4000 B fluorescent microscope before being photographed on a Zeiss LSM 510 laser scanning confocal microscope (Carl Zeiss, Thornwood, NY) using 543 nm helium−neon laser or 488 nm argon laser to view Alexa Fluor conjugates. Emissions were collected using 480−520 nm and 500−615 nm band-pass filters (BP565-615, Carl Zeiss AG) through a 10× 0.45 NA objective (Plan-Apochromat SF25, Carl Zeiss AG), 25× 0.80 NA objective (LCI Plan-Neofluar, Carl Zeiss AG), or 40× 0.95 NA objective (Plan-


DOI: 10.1021/acschemneuro.8b00021
ACS Chem. Neurosci. 2018, 9, 2074−2088

Apochromat M27, Carl Zeiss AG). Confocal z-stacks of sections ranged from 30 to 60 μm depth (depending on thickness of cryosection). Whole-mount confocal images were more variable, but care was taken to ensure that z-stacks also included several scans above and below the regions of interest to ensure that the entire subject was captured. The distance between optical sections was set using optimal interval settings suggested by the acquisition software. Z-stacks were converted into maximum intensity or standard deviation projections using Fiji (ImageJ v3.2.1 for Mac OS X, National Institute of Health, Bethesda, MD[94]) and Zeiss ZEN2009 software.

IHC involving DAB staining and ISH involving BCIP/NBT staining were viewed under a Leica DMLB microscope and imaged using a Qimaging Retiga 2000R camera. Final figures were constructed using Adobe Photoshop CC 2015 (Adobe Systems, Inc., San Jose, CA) and Fiji with adjustments for size, contrast, and brightness. Schematic diagrams were drawn using Adobe Photoshop CC 2015.

**Data Analysis.** Numerical values, such as neuron diameter, were measured with Fiji using scale information captured by Zeiss ZEN2009 software. Values are expressed as mean ± standard deviation ($n$ = specimen). Scale bars in figures were also calculated via Zeiss ZEN2009 and Fiji software.

## AUTHOR INFORMATION


### Corresponding Author

*E-mail: baratte@mnhn.fr.

### ORCID

Roger P. Croll: 0000-0002-9846-0923


### Author Contributions

The manuscript has been read and approved by all named authors, and there are no other persons who satisfied the criteria for authorship but are not listed. We further confirm that the order of authors listed in the manuscript has been approved by all of us. All authors had full access to all the data in the study and take responsibility for the integrity of the data and the accuracy of the data analysis. Acquisition of data: A.T.S., S.B., and R.P.C. Analysis and interpretation of data: A.T.S., S.B., and R.P.C. Drafting of the manuscript: A.T.S., S.B., and R.P.C. Critical revision of the manuscript for important intellectual content: A.T.S., R.P.C., and S.B.


### Funding

Natural Sciences and Engineering Research Council of Canada, Laboratoire Biologie des Organismes et Ecosystémes Aquatiques in Paris (Le Centre National de la Recherche Scientifique, UMR 7208, Museum National d'Histoire Naturelle, Institut de Recherche pour le Developement France, 207, Université Pierre et Marie Curie), the France Canada Research Fund (2013), the Mitacs Globalink Research Program (2015), the province of Nova Scotia for the Graduate Scholarship (2017), and Dalhousie University for the International Differential Fee Scholarship (2017).


### Notes

The authors declare no competing financial interest.

## ACKNOWLEDGMENTS


We thank the Biologie des Organismes et EEcosystèmes Aquatiques (BOREA) team in Paris for their assistance with in situ hybridization, cryostections, and collaboration: Drs. Aude Andouche, Laure Bonnaud, Yann Bassaglia; and Boudjema Imarazene and Antoine Rio-Cabello. La Station Marine de Concarneau, particularly Drs. Stephanie Auzoux-Bordenave and Aicha Badou for hosting us annually over the last several years for specimen collection. Drs. Alex Quinn, Paivi Torkkeli, Alan Fine, and Shelley Adamo for being part of the M.Sc. supervisory committee for A.S. The Croll lab, specifically Jillian Doyle, Neil Merovitch, Arnaud Gaudin, Griffin Beach, Matt Stoyek, and all the undergraduate volunteers for all their help and advice.


## ABBREVIATIONS

5-HT, serotonin; AcTub, acetylated α-tubulin; AP, alkaline phosphatase; APGWa, APGWamide (Ala-Pro-Gly-Trp-$NH_2$); BCIP, 5-bromo-4-chloro-30-indolyphosphate p-toluidine salt; cDNA, complementary DNA; CUBIC, clear, unobstructed brain/body imaging cocktail; DAB, 3,3′-diaminobenzidine; DIG, digoxigen; DiI, (2$Z$)-2-[($E$)-3-(3,3-dimethyl-1-octadecylindol-1-ium-2-yl) prop-2-enylidene]-3,3-dimethyl-1-octadecylindole perchlorate; $dH_2O$, distilled water; DMSO, dimethyl sulfoxide; EDAC, 1-ethyl-3(3-dimethylaminopropyl)-carbodiimide; F-actin, filamentous actin; FMRFa, FMRFamide (Phe-Met-Arg-Phe-$NH_2$); FaRPs, FMRFamide-related peptides; HA, histamine; IHC, immunohistochemistry; ISH, in situ hybridization; LIR, like immunoreactive; MABT, maleic acid buffer containing Tween 20; NOS, nitric oxide synthase; Olf E, olfactory epithelium; Olf O, olfactory organ; OSN, olfactory sensory neuron; PBS, phosphate buffer saline; PBS-Tx, phosphate buffer saline with Triton X-100; PCR, polymerase chain reaction; PFA, paraformaldehyde; RNA, ribonucleic acid; RNase, ribonuclease

## REFERENCES


(1) Godfrey-Smith, P. (2016) *Other minds: The Octopus, the sea, and the deep origins of consciousness*, Farrar, Straus and Giroux.

(2) Kölliker, A. (1844) *Entwickelungsgeschichte der Cephalopoden*, p 176, Vol. 6, Meyer u. Zeller, Zürich10.5962/bhl.title.4786.

(3) Young, J. Z. (1936) The structure of nerve fibres in cephalopods and Crustacea. *Proc. R. Soc. London, Ser. B 121*, 319−337.

(4) Hodgkin, A. L., and Huxley, A. F. (1939) Action potentials recorded from inside a nerve fibre. *Nature 144*, 710−711.

(5) Wells, M. (1963) Taste by touch: Some experiments with Octopus. *J. Exp. Biol. 40*, 187−193.

(6) Messenger, J. (1979) The nervous system of *Loligo*: IV the peduncle and olfactory lobes. *Philos. Trans. R. Soc., B 285*, 275−309.

(7) Packard, A. (1972) Cephalopods and fish: the limits of convergence. *Biol. Rev. 47*, 241−307.

(8) Serb, J. M., and Eernisse, D. J. (2008) Charting evolution's trajectory: using molluscan eye diversity to understand parallel and convergent evolution. *Evo. Ed. Outreach 1*, 439−447.

(9) Yoshida, M. A., Yura, K., and Ogura, A. (2015) Cephalopod eye evolution was modulated by the acquisition of Pax-6 splicing variants. *Sci. Rep. 4*, 42−56.

(10) Eisthen, H. L. (2002) Why are olfactory systems of different animals so similar? *Brain Behav. Evol. 59*, 273−293.

(11) Hildebrand, J. G., and Shepherd, G. M. (1997) Mechanisms of olfactory discrimination: Converging evidence for common principles across phyla. *Annu. Rev. Neurosci. 20*, 595−631.

(12) Benton, R., Vannice, K. S., Gomez-Diaz, C., and Vosshall, L. B. (2009) Variant ionotropic glutamate receptors as chemosensory receptors in *Drosophila*. *Cell 136*, 149−162.

(13) Halasz, N., and Shepherd, G. (1983) Neurochemistry of the vertebrate olfactory bulb. *Neuroscience 10*, 579−619.

(14) Hansson, B. S., and Anton, S. (2000) Function and morphology of the antennal lobe: New developments. *Annu. Rev. Entomol. 45*, 203−231.

(15) Ache, B. W., and Young, J. M. (2005) Olfaction: Diverse species, conserved principles. *Neuron 48*, 417−430.

(16) Heuer, C. M., Müller, C. H., Todt, C., and Loesel, R. (2010) Comparative neuroanatomy suggests repeated reduction of neuroarchitectural complexity in Annelida. *Front. Zool. 7*, 13.

(17) Croll, R. P. (1983) Gastropod chemoreception. *Biol. Rev. 58*, 293−319.




DOI: 10.1021/acschemneuro.8b00021
*ACS Chem. Neurosci.* 2018, 9, 2074−2088

(18) Cummins, S. F., and Wyeth, R. C. (2014) Olfaction in gastropods. In *Neuroecology and Neuroethology in Molluscs: The Interface between Behaviour and Environment* (Di Cosmo, A., and Winlow, W., Eds.), 1st ed., pp 45−72, Nova Science Publishers, Inc., New York.
(19) Chase, R., and Tolloczko, B. (1986) Synaptic glomeruli in the olfactory system of a snail. *Cell Tissue Res. 246*, 567−573.
(20) Ito, I., Nakamura, H., Kimura, T., Suzuki, H., Sekiguchi, T., Kawabata, K., and Ito, E. (2000) Neuronal components of the superior and inferior tentacles in the terrestrial slug. *Neurosci. Res. 37*, 191−200.
(21) Croll, R. P., Boudko, D. Y., Pires, A., and Hadfield, M. G. (2003) Transmitter contents of cells and fibers in the cephalic sensory organs of the gastropod mollusc *Phestilla sibogae*. *Cell Tissue Res. 314*, 437−448.
(22) Moroz, L. L. (2006) Localization of putative nitrergic neurons in peripheral chemosensory areas and the central nervous system of *Aplysia californica*. *J. Comp. Neurol. 495*, 10−20.
(23) Wertz, A., Rössler, W., Obermayer, M., and Bickmeyer, U. (2006) Functional neuroanatomy of the rhinophore of *Aplysia punctata*. *Front. Zool. 3*, 6.
(24) Wertz, A., Rössler, W., Obermayer, M., and Bickmeyer, U. (2007) Functional neuroanatomy of the rhinophore of *Archidoris pseudoargus*. *Helgol. Mar. Res. 61*, 135−142.
(25) Göbbeler, K., and Klussmann-Kolb, A. (2007) A comparative ultrastructural investigation of the cephalic sensory organs in Opisthobranchia (Mollusca, Gastropoda). *Tissue Cell 39*, 399−414.
(26) Faller, S., Staubach, S., and Klussmann-Kolb, A. (2008) Comparative immunohistochemistry of the cephalic sensory organs in Opisthobranchia (Mollusca, Gastropoda). *Zoomorphology. 127*, 227−239.
(27) Gaudin, A., and Gascuel, J. (2005) 3D atlas describing the ontogenic evolution of the primary olfactory projections in the olfactory bulb of *Xenopus laevis*. *J. Comp. Neurol. 489*, 403−424.
(28) Messenger, J. B. (1967) The peduncle lobe: A visuo-motor centre in Octopus. *Proc. R. Soc. London, Ser. B 167*, 225−251.
(29) Budelmann, B. U. (1995) Cephalopod sense organs, nerves and the brain: Adaptations for high performance and life style. *Mar. Freshwater Behav. Physiol. 25*, 13−33.
(30) Mobley, A. S., Michel, W. C., and Lucero, M. T. (2008) Odorant responsiveness of squid olfactory receptor neurons. *Anat. Rec. 291*, 763−774.
(31) Walderon, M. D., Nolt, K. J., Haas, R. E., Prosser, K. N., Holm, J. B., Nagle, G. T., and Boal, J. G. (2011) Distance chemoreception and the detection of conspecifics in *Octopus bimaculoides*. *J. Mollusc. Stud. 77*, 309−311.
(32) Barber, V., and Wright, D. (1969) The fine structure of the sense organs of the cephalopod mollusc *Nautilus*. *Cell Tissue Res. 102*, 293−312.
(33) Ruth, P., Schmidtberg, H., Westermann, B., and Schipp, R. (2002) The sensory epithelium of the tentacles and the rhinophore of *Nautilus pompilius L.* (Cephalopoda, Nautiloidea). *J. Morphol. 251*, 239−255.
(34) Woodhams, M. P., and Messenger, J. (1974) A note on the ultrastructure of the *Octopus* olfactory organ. *Cell Tissue Res. 152*, 253−258.
(35) Shigeno, S., and Yamamoto, M. (2002) Organization of the nervous system in the pygmy cuttlefish, *Idiosepius paradoxus Ortmann* (Idiosepiidae, Cephalopoda). *J. Morphol. 254*, 65−80.
(36) Young, J. Z. (1965) The central nervous system of *Nautilus*. *Philos. Trans. R. Soc., B 249*, 1−25.
(37) Young, J. Z. (1971) *Anatomy of the nervous system of Octopus vulgaris*, Clarendon Press, Oxford.
(38) Di Cristo, C., Van Minnen, J., and Di Cosmo, A. (2005) The presence of APGWamide in *Octopus vulgaris*: a possible role in the reproductive behavior. *Peptides 26*, 53−62.
(39) Di Cristo, C., De Lisa, E., and Di Cosmo, A. (2009) Control of GnRH expression in the olfactory lobe of *Octopus vulgaris*. *Peptides 30*, 538−544.
(40) Polese, G., Bertapelle, C., and Di Cosmo, A. (2015) Role of olfaction in *Octopus vulgaris* reproduction. *Gen. Comp. Endocrinol. 210*, 55−62.
(41) Buresi, A., Andouche, A., Navet, S., Bassaglia, Y., Bonnaud-Ponticelli, L., and Baratte, S. (2016) Nervous system development in cephalopods: How egg yolk-richness modifies the topology of the mediolateral patterning system. *Dev. Biol. 415*, 143−156.
(42) Buresi, A., Croll, R. P., Tiozzo, S., Bonnaud, L., and Baratte, S. (2014) Emergence of sensory structures in the developing epidermis in *Sepia officinalis* and other coleoid cephalopods. *J. Comp. Neurol. 522*, 3004−3019.
(43) Shigeno, S., Parnaik, R., Albertin, C. B., and Ragsdale, C. W. (2015) Evidence for a cordal, not ganglionic, pattern of cephalopod brain neurogenesis. *Zool. Lett. 1*, 26.
(44) Oland, L. A., and Tolbert, L. P. (1998) Glomerulus development in the absence of a set of mitral-like neurons in the insect olfactory lobe. *J. Neurobiol. 36*, 41−52.
(45) Pinelli, C., D'Aniello, B., Polese, G., and Rastogi, R. K. (2004) Extrabulbar olfactory system and nervus terminalis FMRFamide immunoreactive components in *Xenopus laevis* ontogenesis. *J. Chem. Neuroanat. 28*, 37−46.
(46) Wyeth, R. C., and Croll, R. P. (2011) Peripheral sensory cells in the cephalic sensory organs of *Lymnaea stagnalis*. *J. Comp. Neurol. 519*, 1894−1913.
(47) Baratte, S., and Bonnaud, L. (2009) Evidence of early nervous differentiation and early catecholaminergic sensory system during *Sepia officinalis* embryogenesis. *J. Comp. Neurol. 517*, 539−549.
(48) Wollesen, T., Loesel, R., and Wanninger, A. (2009) Pygmy squids and giant brains: Mapping the complex cephalopod CNS by phalloidin staining of vibratome sections and whole-mount preparations. *J. Neurosci. Methods 179*, 63−67.
(49) Rawlinson, K. A. (2010) Embryonic and post-embryonic development of the polyclad flatworm *Maritigrella crozieri*; implications for the evolution of spiralian life history traits. *Front. Zool. 7*, 12.
(50) Wanninger, A., Ruthensteiner, B., and Haszprunar, G. (2000) Torsion in *Patella caerulea* (Mollusca, Patellogastropoda): ontogenetic process, timing, and mechanisms. *Invertebr. Biol. 119*, 177−187.
(51) Rossler, W., Kuduz, J., Schurmann, F. W., and Schild, D. (2002) Aggregation of f-actin in olfactory glomeruli: A common feature of glomeruli across phyla. *Chem. Sens. 27*, 803−810.
(52) Shigeno, S., Kidokoro, H., Tsuchiya, K., Segawa, S., and Yamamoto, M. (2001) Development of the brain in the oegopsid squid, *Todarodes pacificus*: An atlas up to the hatching stage. *Zool. Sci. 18*, 527−541.
(53) Wildenburg, G. (1997) Structure of the so-called olfactory organ of octopods after hatching: evidence for its chemoreceptive function. *Vie Mileiu 47*, 137−142.
(54) Polese, G., Bertapelle, C., and Di Cosmo, A. (2016) Olfactory organ of *Octopus vulgaris*: morphology, plasticity, turnover and sensory characterization. *Biol. Open 5*, 611.
(55) Emery, D. G. (1975) The histology and fine structure of the olfactory organ of the squid *Lolliguncula brevis blainville*. *Tissue Cell 7*, 357−367.
(56) Darmaillacq, A., Lesimple, C., and Dickel, L. (2008) Embryonic visual learning in the cuttlefish. *Anim. Behav. 76*, 131−134.
(57) Romagny, S., Darmaillacq, A. S., Guibe, M., Bellanger, C., and Dickel, L. (2012) Feel, smell and see in an egg: Emergence of perception and learning in an immature invertebrate, the cuttlefish embryo. *J. Exp. Biol. 215*, 4125−4130.
(58) Graziadei, P. (1962) Receptors in the suckers of *Octopus*. *Nature 195*, 57−59.
(59) Campinho, M. A., Oliveira, A. R., and Sykes, A. V. (2017) Olfactory-like neurons are present in the forehead of common cuttlefish, *Sepia officinalis* Linnaeus, 1758 (Cephalopoda: Sepiidae). *Zool. J. Linnean Soc. 20*, 1−9.
(60) Di Cristo, C., Bovi, P. D., and Di Cosmo, A. (2003) Role of FMRFamide in the reproduction of *Octopus vulgaris*: molecular analysis and effect on visual input. *Peptides 24* (10), 1525−1532.


DOI: 10.1021/acschemneuro.8b00021
*ACS Chem. Neurosci.* 2018, 9, 2074−2088

(61) Di Cosmo, A., and Di Cristo, C. (1998) Neuropeptidergic control of the optic gland of *Octopus vulgaris*: FMRF-amide and GnRH immunoreactivity. *J. Comp. Neurol. 398*, 1−12.
(62) Di Cosmo, A., Di Cristo, C., Palumbo, A., d'Ischia, M., and Messenger, J. B. (2000) Nitric oxide synthase (NOS) in the brain of the cephalopod *Sepia officinalis*. *J. Comp. Neurol. 428*, 411−427.
(63) Elphick, M. R., Kemenes, G., Staras, K., and O'Shea, M. (1995) Behavioral role for nitric oxide in chemosensory activation of feeding in a mollusc. *J. Neurosci. 15*, 7653−7664.
(64) Hegedűs, E., Kaslin, J., Hiripi, L., Kiss, T., Panula, P., and Elekes, K. (2004) Histaminergic neurons in the central and peripheral nervous system of gastropods (*Helix, Lymnaea*): An immunocytochemical, biochemical, and electrophysiological approach. *J. Comp. Neurol. 475*, 391−405.
(65) Habib, M. R., Mohamed, A. H., Osman, G. Y., El-Din, A. T. S., Mossalem, H. S., Delgado, N., Torres, G., Rolon-Martinez, S., Miller, M. W., and Croll, R. P. (2015) Histamine immunoreactive elements in the central and peripheral nervous systems of the snail, *Biomphalaria spp.*, intermediate host for *Schistosoma mansoni*. *PLoS One 10*, e0129800.
(66) Suzuki, H., Kimura, T., Sekiguchi, T., and Mizukami, A. (1997) FMRFamide-like-immunoreactive primary sensory neurons in the olfactory system of the terrestrial mollusc. *Cell Tissue Res. 289*, 339−345.
(67) Nezlin, L., and Voronezhskaya, E. (1997) GABA-immunoreactive neurones and interactions of GABA with serotonin and FMRFamide in a peripheral sensory ganglion of the pond snail *Lymnaea stagnalis*. *Brain Res. 772*, 217−225.
(68) Messenger, J. B. (1996) Neurotransmitters of cephalopods. *Invertebr. Neurosci. 2*, 95−114.
(69) Wollesen, T., Degnan, B. M., and Wanninger, A. (2010) Expression of serotonin (5-HT) during CNS development of the cephalopod mollusk. *Cell Tissue Res. 342*, 161−178.
(70) Moroz, L. L., Sudlow, L. C., Jing, J., and Gillette, R. (1997) Serotonin-immunoreactivity in peripheral tissues of the opisthobranch molluscs *Pleurobranchaea californica* and *Tritonia diomedea*. *J. Comp. Neurol. 382*, 176−188.
(71) Shigeno, S., Tsuchiya, K., and Segawa, S. (2001) Embryonic and paralarval development of the central nervous system of the loliginid squid *Sepioteuthis lessoniana*. *J. Comp. Neurol. 437*, 449−475.
(72) Zatylny-Gaudin, C., and Favrel, P. (2014) Diversity of the -RFamide peptide family in mollusks. *Front. Endocrinol. 5*, 178.
(73) Graziadei, P. P. C., and Graziadei, G. M. (1980) Neurogenesis and neuron regeneration in the olfactory system of mammals. III. Deafferentation and reinnervation of the olfactory bulb following section of the *fila olfactoria* in rat. *J. Neurocytol. 9*, 145−162.
(74) Dehmelt, L., and Halpain, S. (2004) Actin and microtubules in neurite initiation: are MAPs the missing link? *J. Neurobiol. 58*, 18−33.
(75) Kishida, T., Thewissen, J. G. M., Hayakawa, T., Imai, H., and Agata, K. (2015) Aquatic adaptation and the evolution of smell and taste in whales. *Zool. Lett. 1*, 9.
(76) Strausfeld, N. J., and Hildebrand, J. G. (1999) Olfactory systems: common design, uncommon origins? *Curr. Opin. Neurobiol. 9*, 634−639.
(77) Liscovitch-Brauer, N., Alon, S., Porath, H. T., Elstein, B., Unger, R., Ziv, T., Admon, A., Levanon, E. Y., Rosenthal, J. J. C., and Eisenberg, E. (2017) Trade-off between transcriptome plasticity and genome evolution in cephalopods. *Cell 169*, 191−202.
(78) Mori, K., Nagao, H., and Yoshihara, Y. (1999) The olfactory bulb: coding and processing of odor molecule information. *Science 286*, 711−715.
(79) Lemaire, J. (1970) Table de développement embryonnaire de *Sepia officinalis L.* (mollusque céphalopode). *Bull. Soc. Zool. Fr. 95*, 773−782.
(80) Yamamoto, M., Shimazaki, Y., and Shigeno, S. (2003) Atlas of the embryonic brain in the pygmy squid. *Zool. Sci. 20*, 163−179.
(81) Panula, P., Häppölä, O., Airaksinen, M. S., Auvinen, S., and Virkamäki, A. (1988) Carbodiimide as a tissue fixative in histamine immunohistochemistry and its application in developmental neurobiology. *J. Histochem. Cytochem. 36*, 259−269.
(82) Croll, R. P. (2006) Development of embryonic and larval cells containing serotonin, catecholamines, and FMRFamide-related peptides in the gastropod mollusc *Phestilla sibogae*. *Biol. Bull. 211*, 232.
(83) Susaki, E. A., Tainaka, K., Perrin, D., Yukinaga, H., Kuno, A., and Ueda, H. R. (2015) Advanced CUBIC protocols for whole-brain and whole-body clearing and imaging. *Nat. Protoc. 10*, 1709−1727.
(84) Howes, S. C., Alushin, G. M., Shida, T., Nachury, M. V., and Nogales, E. (2014) Effects of tubulin acetylation and tubulin acetyltransferase binding on microtubule structure. *Mol. Biol. Cell 25*, 257−266.
(85) Todt, C., Büchinger, T., and Wanninger, A. (2008) The nervous system of the basal mollusk *Wirenia argentea* (Solenogastres): a study employing immunocytochemical and 3D reconstruction techniques. *Mar. Biol. Res. 4*, 290−303.
(86) Mattiello, T., Costantini, M., Di Matteo, B., Livigni, S., Andouche, A., Bonnaud, L., and Palumbo, A. (2012) The dynamic nitric oxide pattern in developing cuttlefish *Sepia officinalis*. *Dev. Dyn. 241*, 390−402.
(87) McCann, C. J., Hwang, S. J., Hennig, G. W., Ward, S. M., and Sanders, K. M. (2014) Bone marrow derived Kit-positive cells colonize the gut but fail to restore pacemaker function in intestines lacking interstitial cells of Cajal. *Neurogastroenterol. Motility. 20*, 326.
(88) Stenesen, D., Moehlman, A. T., and Krämer, H. (2015) The carcinine transporter CarT is required in *Drosophila* photoreceptor neurons to sustain histamine recycling. *eLife 4*, No. e10972.
(89) Matsuo, R., Fukata, R., Kumagai, M., Kobayashi, A., Kobayashi, S., and Matsuo, Y. (2016) Distribution of histaminergic neurons and their modulatory effects on oscillatory activity in the olfactory center of the terrestrial slug *Limax*. *J. Comp. Neurol. 524*, 119−135.
(90) Röszer, T., Jenei, Z., Gáll, T., Nagy, O., Czimmerer, Z., Serfözö, Z., Elekes, K., and Bánfalvi, G. (2003) A possible stimulatory effect of FMRFamide on neural nitric oxide production in the central nervous system of *Helix lucorum L.* *Brain Behav. Evol. 63*, 23−33.
(91) Croll, R. P., and Van Minnen, J. (1992) Distribution of the peptide Ala-Pro-Gly-Trp-NH2 (APGWamide) in the nervous system and periphery of the snail *Lymnaea stagnalis* as revealed by immunocytochemistry and in situ hybridization. *J. Comp. Neurol. 324*, 567−574.
(92) Fan, X., Croll, R. P., Wu, B., Fang, L., Shen, Q., Painter, S. D., and Nagle, G. T. (1997) Molecular cloning of a cDNA encoding the neuropeptides APGWamide and cerebral peptide 1: Localization of APGWamide-like immunoreactivity in the central nervous system and male reproductive organs of *Aplysia*. *J. Comp. Neurol. 387*, 53−62.
(93) Smith, S., Nason, J., and Croll, R. (1997) Detection of APGWamide-like immunoreactivity in the sea scallop. *Neuropeptides 31*, 155−165.
(94) Schindelin, J., Arganda-Carreras, I., Frise, E., Kaynig, V., Longair, M., Pietzsch, T., and Schmid, B. (2012) Fiji: An open-source platform for biological-image analysis. *Nat. Methods 9*, 676−682.


DOI: 10.1021/acschemneuro.8b00021
*ACS Chem. Neurosci.* 2018, 9, 2074−2088